University of Strathclyde
Engineering

Novel Nanoparticle Cement

for crack sealing and water transport:

from structural study to lab-scale application

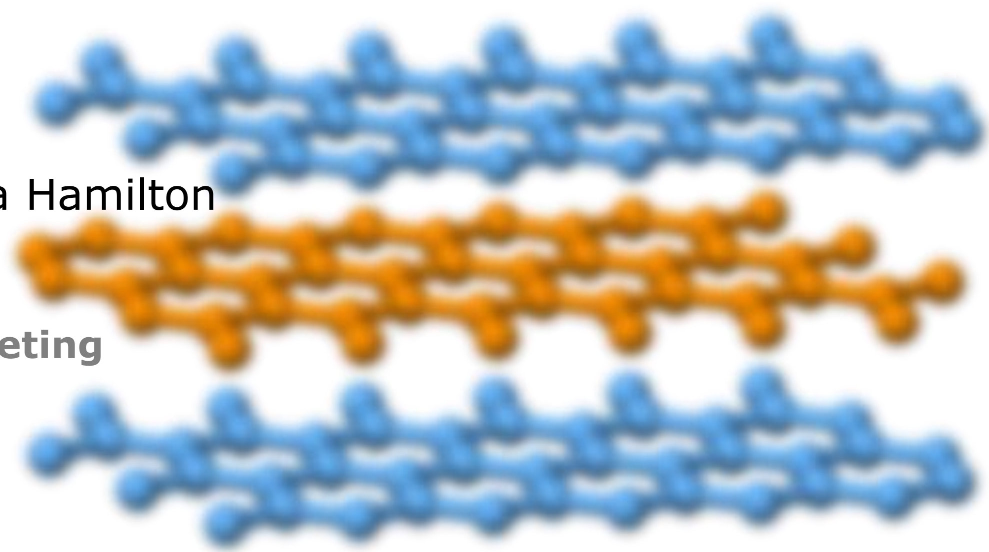

Riccardo Maddalena, Dr Andrea Hamilton
University of Strathclyde, UK

Theme 4 – Structural Integrity Meeting
14th November 2016
Penrith UK

DISTINCTIVE   NATIONAL NUCLEAR LABORATORY   Sellafield Ltd   NDA Nuclear Decommissioning Authority

GANTT Chart

University of Strathclyde Engineering

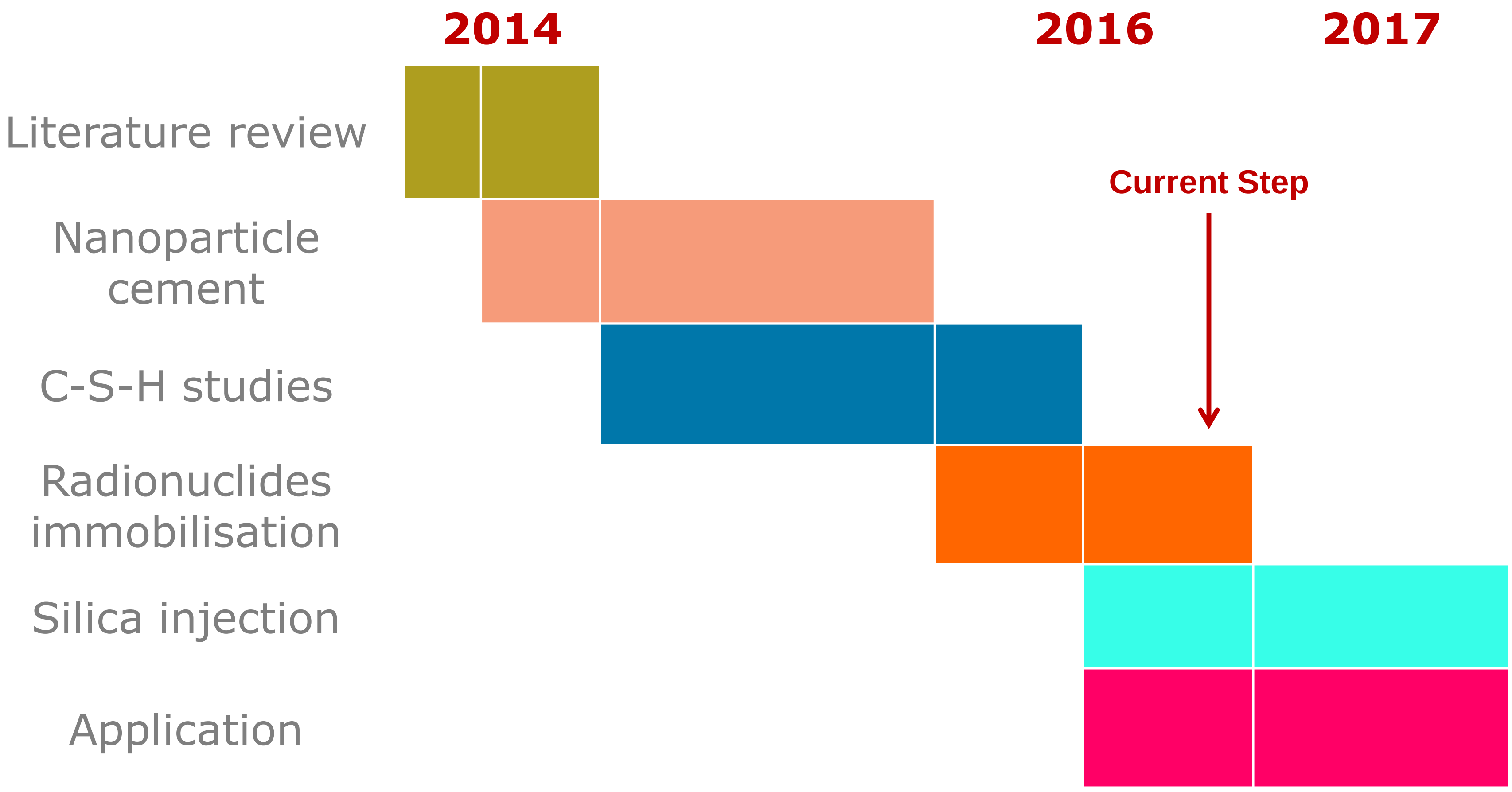

DISTINCTIVE

NATIONAL NUCLEAR LABORATORY

Sellafield Ltd

NDA Nuclear Decommissioning Authority

INTRODUCTION

NANOPARTICLE CEMENT

C-S-H STRUCTURAL STUDY

RADIONUCLIDE IMMOBILIZATION

LOW PRESSURE NANOSILICA INJECTION

FUTURE WORK

Introduction
Structural Integrity

University of Strathclyde
Engineering

Deterioration of concrete and its durability has been the main concern in the last decades

[J. Collins 2010 - www.bridgehunter.com]

[Engineering and Technical Consultants, 2010]

DISTINCTIVE   NATIONAL NUCLEAR LABORATORY   Sellafield Ltd   NDA Nuclear Decommissioning Authority

Introduction
Structural Integrity

- Chemical attack due to chlorides or other corrosive compounds
- Freeze and thaw cycles exposition
- Erosion due to saline environment
- High moisture transport through concrete elements

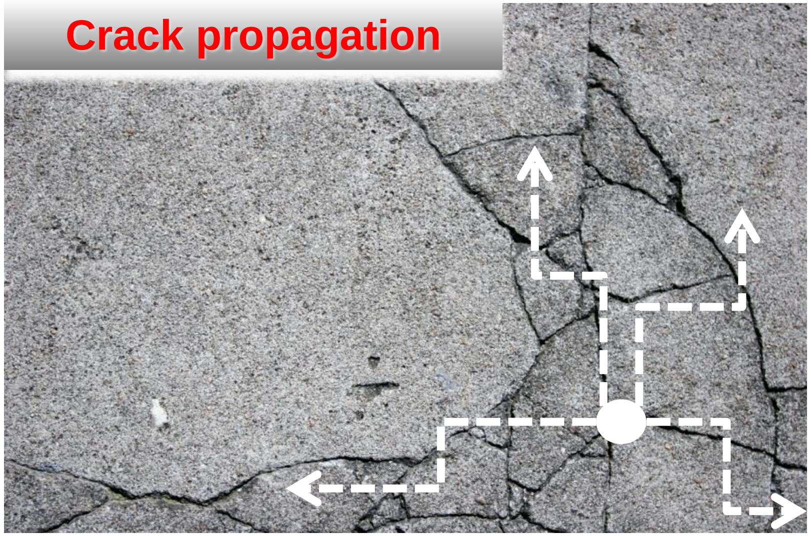

The main effect is the formation of nano-micro-macro-**dangerous** cracks. Those can in turn involve several reactions, increasing the moisture content, air entrainment, contamination flux and compromise the safety, standard conformity and workability of the concrete structures.

DISTINCTIVE

NATIONAL NUCLEAR LABORATORY

Sellafield Ltd

NDA Nuclear Decommissioning Authority

Nanoparticle cement

Nanoparticle materials have been studied in concrete science: they act as a *filler*, reducing the water penetration content (or other potential contaminants), improving compressive strength, and enhancing the long term durability of concrete.

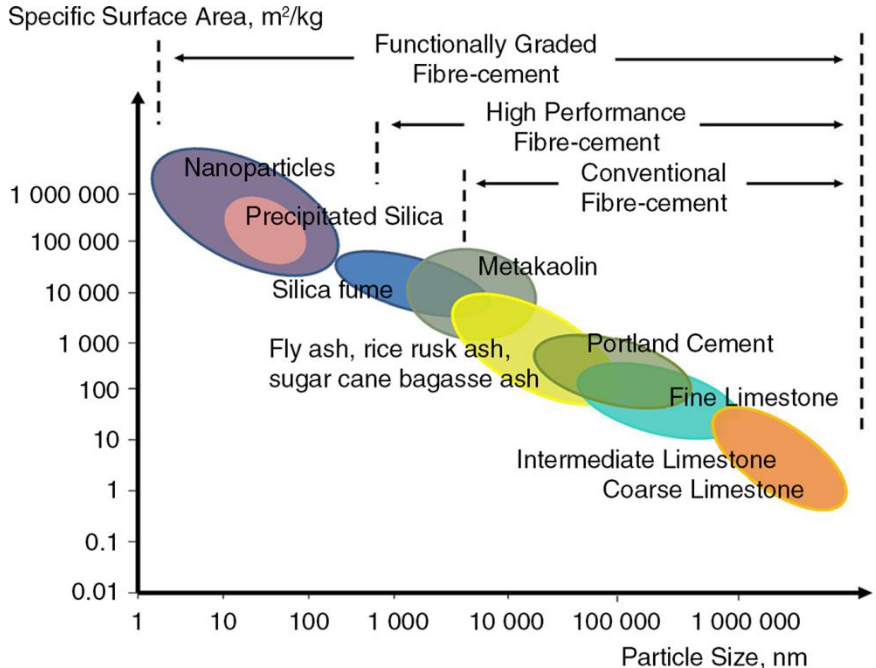

[Sobolev and Gutierrez, 2005]

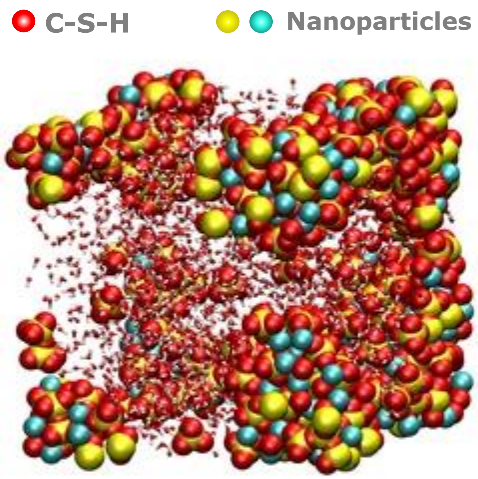

[Griebel, Bonn University, 2010]

DISTINCTIVE NATIONAL NUCLEAR LABORATORY Sellafield Ltd NDA Nuclear Decommissioning Authority

Nanoparticle cement

Sample	Compressive strength			Heat released	Bulk density	Porosity	XRD
	[MPa]			[J/g]	[g/cm^3]	-	phases
	Age [days]						
	3	7	28				
OPC425	16.1	38.4	51.2	235	1.9	0.21	E, P, **CSH**, C, C_3S, C_2S
OPC525	19.2	41.6	63.2	310	1.6	0.35	E, P, **CSH**, C, C_3S, C_2S
CHI	0	2.4	6.4	43	0.9	0.61	P, **CSH**
CHI act	n/a	n/a	n/a	208	1.2	0.49	n/a
MK	0	3.2	5.1	455	1.0	0.53	P, **CSH**, F, Q, NASH
AMK	2.8	8.7	4.6	n/a	0.9	0.59	P, **CAH**, S
BMK	7.5	5.1	6.6	n/a	0.9	0.58	P, **CAH**, **CSH**, S
MK-NS	0.8	1.2	1.8	n/a	0.6	0.72	P, **CSH**, **CAH**, Q, S
3CH-SF	n/a	n/a	n/a	47	n/a	n/a	P, **CSH**
1CH-SF	n/a	n/a	n/a	76	n/a	n/a	P, **CSH**
3CH-NS	n/a	n/a	n/a	151	n/a	n/a	P, **CSH**
1CH-NS	n/a	n/a	n/a	230	n/a	n/a	**CSH**

Research output

Research article

Novel nano-particle cement: from micro-structure to bulk scale

Riccardo Maddalena and Andrea Hamilton

In preparation
Editor: -
Date: November 2016

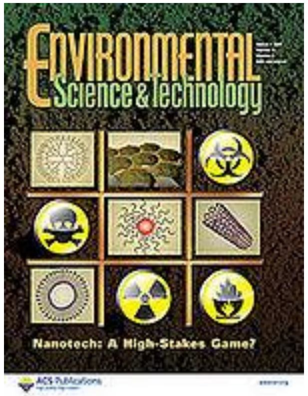

INTRODUCTION

NANOPARTICLE CEMENT

C-S-H STRUCTURAL STUDY

RADIONUCLIDE IMMOBILIZATION

LOW PRESSURE NANOSILICA INJECTION

FUTURE WORK

Calcium Silicate Hydrate

University of Strathclyde Engineering

Calcium-silicate-hydrate (C-S-H) is one of the main results of Portland clinker hydration. It forms by chemical reaction between water and tri- or di-calcium silicate (alite C_3S and belite C_2S respectively), typical clinker minerals.

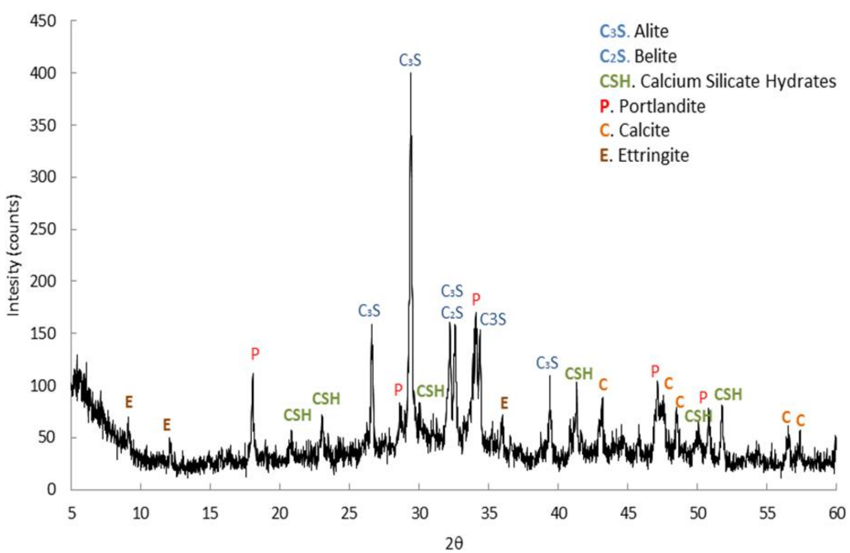

X-Ray diffraction pattern of 13 days aged Ordinary Portland cement.

C-S-H is a gel-like mineral phase, which makes up approximately 2/3 of hydrated Portland cement paste.

It is responsible for ***strength and hardening*** in cement paste and concrete.

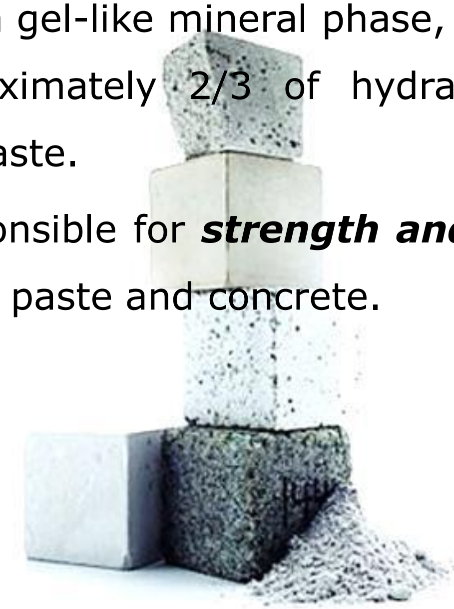

Portlandite

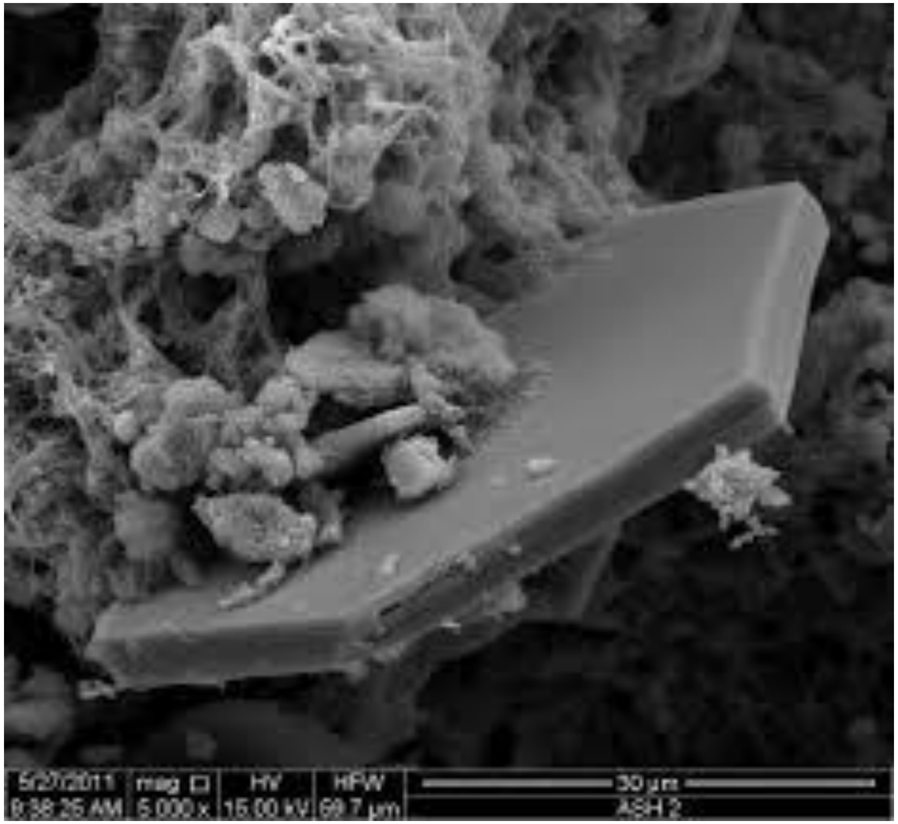

SEM image of Portlandite crystal in hydrated cement [Franus et al., 2005]

Portlandite, $Ca(OH)_2$, is a result of hydrated cement and comes from the reaction of CaO and water.

Portlandite has an hexagonal plate-like structure.

C-S-H synthesis

Synthetic C-S-H was made using two different calcium sources: calcium hydroxide **CH**, reagent grade and calcium oxide **C**, obtained by calcination of calcium carbonate, reagent grade. Two different silica particle sizes were used: silica fume **SF** (0.15 - 0.30 μm) and nanosilica **NS** (5 – 35 nm). Decarbonated water was used in the mixes.

C-S-H paste was manually mixed and cast in cubic moulds. After 24 hours specimens were demoulded and placed in a sealed environment to prevent **carbonation**.

Sample mix	CH	SF	NS	Target ratio
	wt %	wt %	wt %	
CH System				C/S
3CH-SF	75	25	-	>1
1CH-SF	50	50	-	0.81
3CH-NS	75	-	25	>1
1CH-NS	50	-	50	0.81
CO System				C/S
1CO-SF	50	50	-	1.07
1CO-NS	50	-	50	1.07

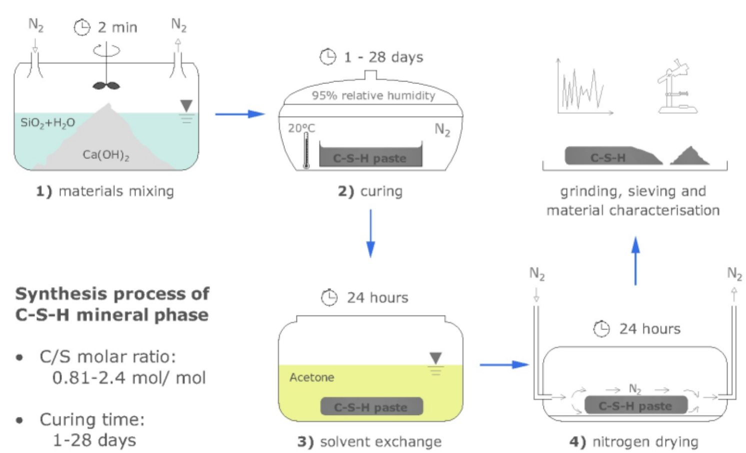

C-S-H Characterization

University of Strathclyde Engineering

Synchrotron X-Ray Diffraction

Monochromatic 2D diffraction, λ = 0.15508 Å

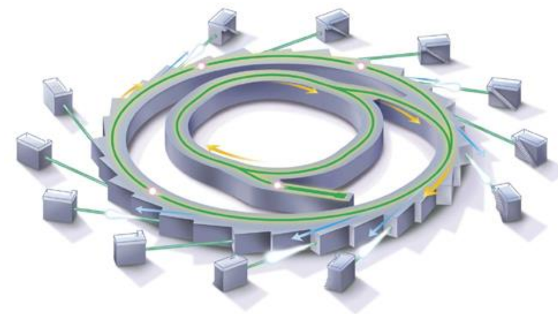

Raman Spectroscopy

100 - 4000 cm^{-1}, 785 nm laser, map size 100 μm grid

Scanning Electron Microscopy

FE-SEM, 20.0 kV and EDX mapping

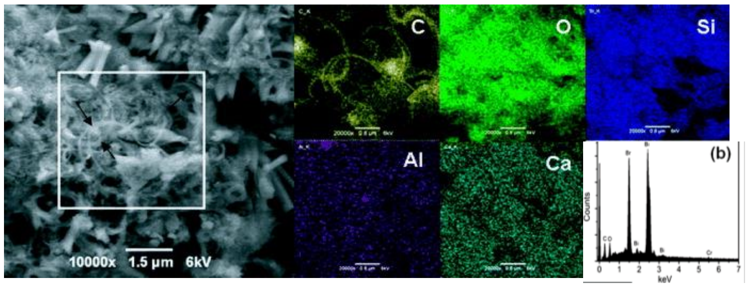

DISTINCTIVE

NATIONAL NUCLEAR LABORATORY

Sellafield Ltd

NDA Nuclear Decommissioning Authority

Research output

University of Strathclyde Engineering

Research article

A novel synthesis process for calcium silicate hydrate gel (C-S-H) with tobermorite-like structure

Riccardo Maddalena and Andrea Hamilton

In submission to **Journal of Material Chemistry A**
Editor: Royal Society of Chemistry
Date: November 2016

Research article

Hydrothermal synthesis of calcium silicate hydrate gel: synchrotron XRD studies

Riccardo Maddalena and Andrea Hamilton

In preparation
Editor: -
Date: December 2016

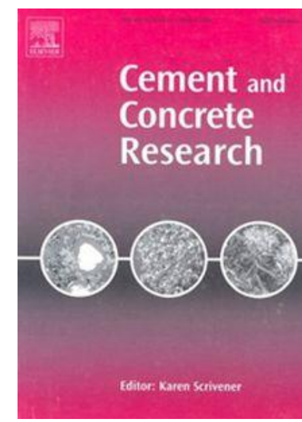

DISTINCTIVE

NATIONAL NUCLEAR LABORATORY

Sellafield Ltd

NDA Nuclear Decommissioning Authority

University of Strathclyde Engineering

INTRODUCTION

NANOPARTICLE CEMENT

C-S-H STRUCTURAL STUDY

RADIONUCLIDE IMMOBILIZATION

LOW PRESSURE NANOSILICA INJECTION

FUTURE WORK

DISTINCTIVE

NATIONAL NUCLEAR LABORATORY

Sellafield Ltd

NDA Nuclear Decommissioning Authority

Radionuclide immobilization

University of Strathclyde Engineering

From previous morphological investigation, C-S-H crystal structural can be altered varying its C/S ratio or synthesis conditions, in order to "**house**" other atoms in its interlayer spacing.

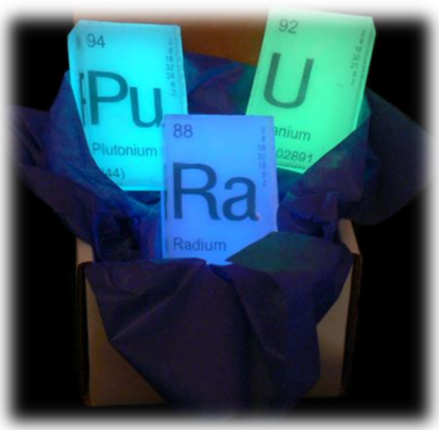

Radionuclides

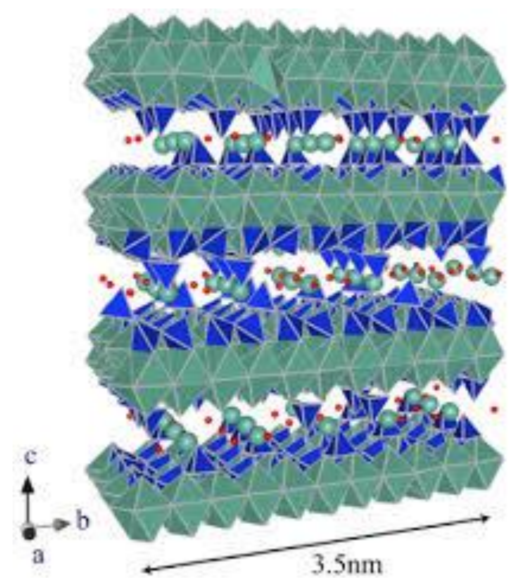

C-S-H

DISTINCTIVE

NATIONAL NUCLEAR LABORATORY

Sellafield Ltd

NDA
Nuclear Decommissioning Authority

Radionuclide immobilization

University of Strathclyde Engineering

[Interaction mechanism of radionuclides with C-S-H phases]

There are three main possible reactions that lead to the immobilisation of radionuclides into the C-S-H structure:

1. complex formation reactions:
   a) outer sphere or b) inner sphere;
2. sorption, ion exchange mechanisms:
   c) structural incorporation;
3. surface precipitation:
   d) co-precipitation.

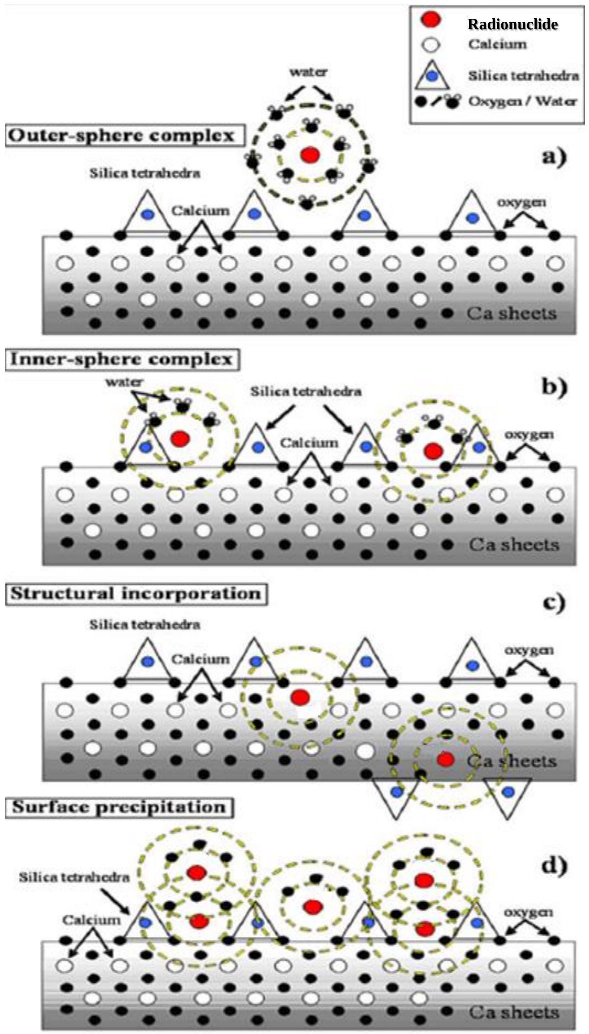

[Mandaliev et al., 2010]

DISTINCTIVE NATIONAL NUCLEAR LABORATORY Sellafield Ltd NDA Nuclear Decommissioning Authority

Radionuclide immobilization

University of Strathclyde Engineering

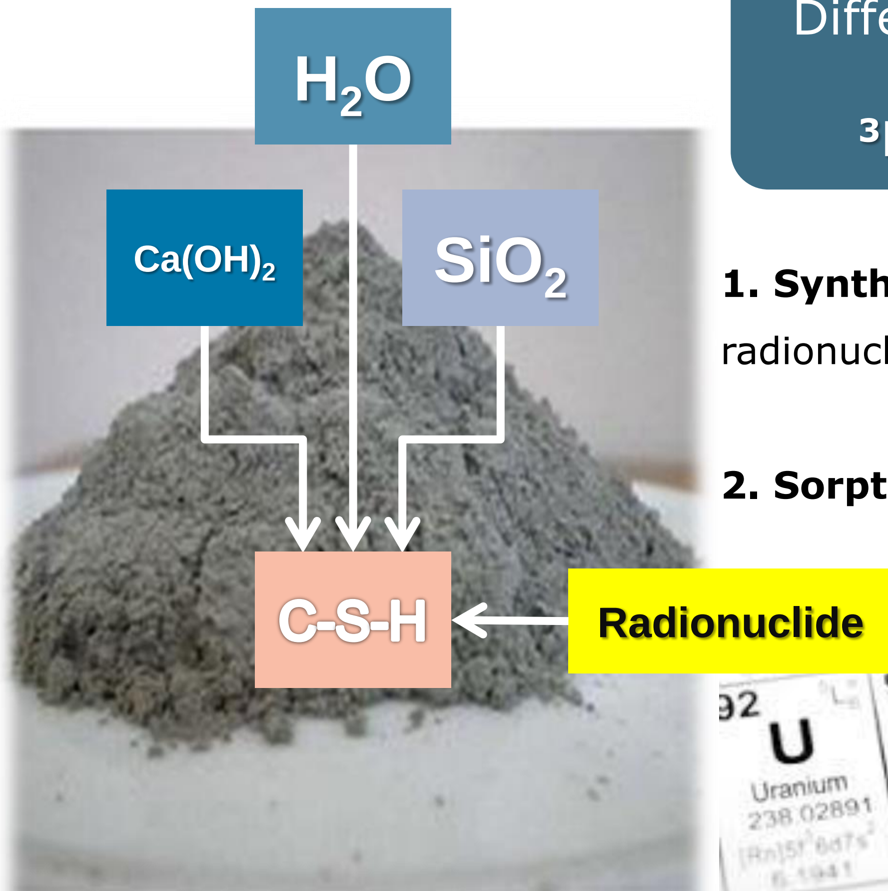

Different radionuclides are investigated:

^{3}H ^{90}Sr ^{99}Tc ^{137}Cs ^{239}Pu ^{232}Th

1. Synthesis and formation of C-S-H phase in presence of radionuclides.

2. Sorption of radionuclides into C-S-H phases with time.

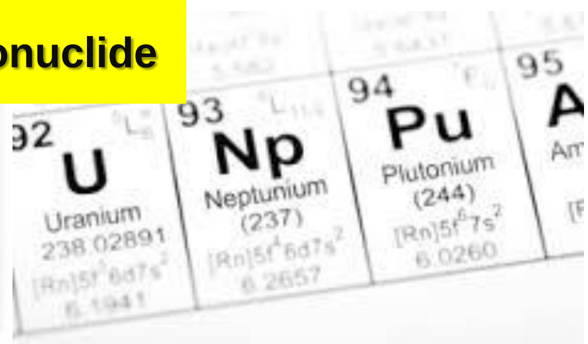

DISTINCTIVE NATIONAL NUCLEAR LABORATORY Sellafield Ltd NDA Nuclear Decommissioning Authority

Radionuclide immobilization

Characterisation of C-S-H paste is the key to fully understand the interaction mechanism of radionuclides with C-S-H phases.

Synchrotron X-Ray Diffraction provides structural information and morphology of C-S-H phases formed in presence of radionuclides.

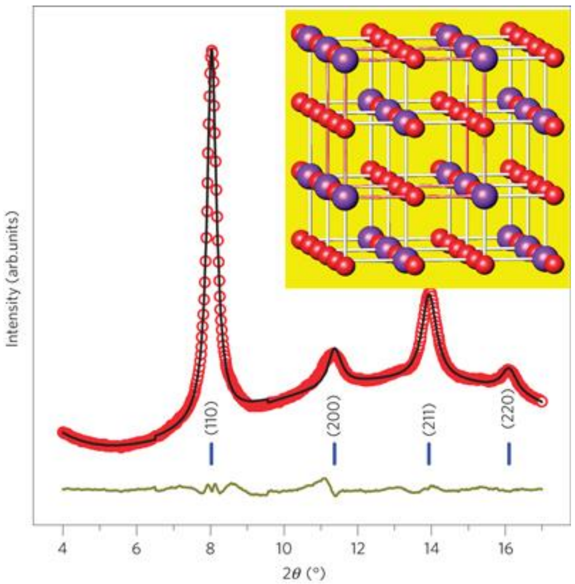

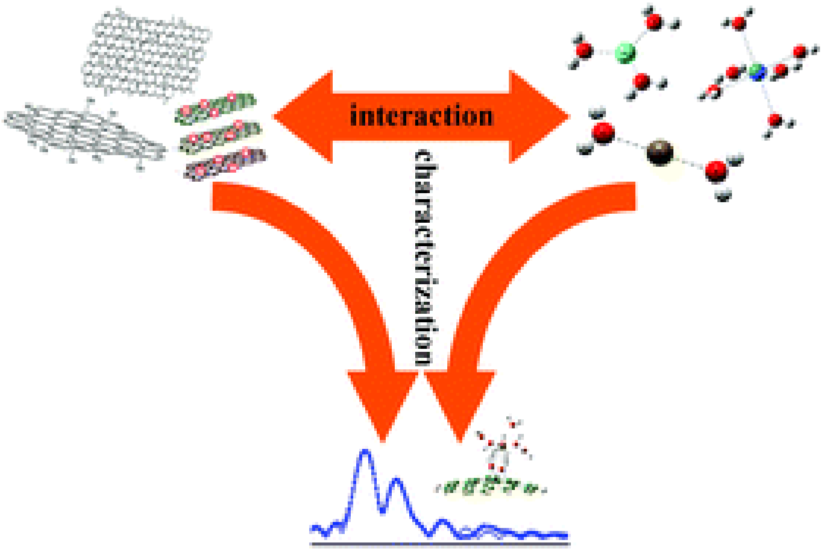

DISTINCTIVE NATIONAL NUCLEAR LABORATORY Sellafield Ltd NDA Nuclear Decommissioning Authority

Radionuclide immobilization

University of Strathclyde Engineering

Characterisation of C-S-H paste is the key to fully understand the interaction mechanism of radionuclides with C-S-H phases.

Sorption test gives quantitative analysis about the immobilisation capability of radionuclides into C-S-H phases

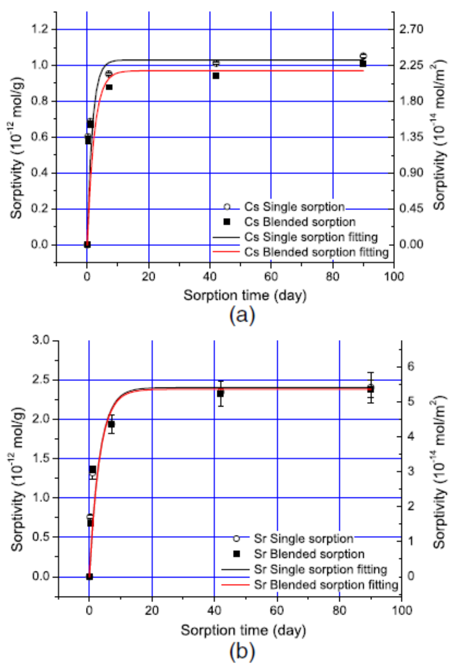

[K. Li, X. Pang, Cement and Concrete Research, 2014]

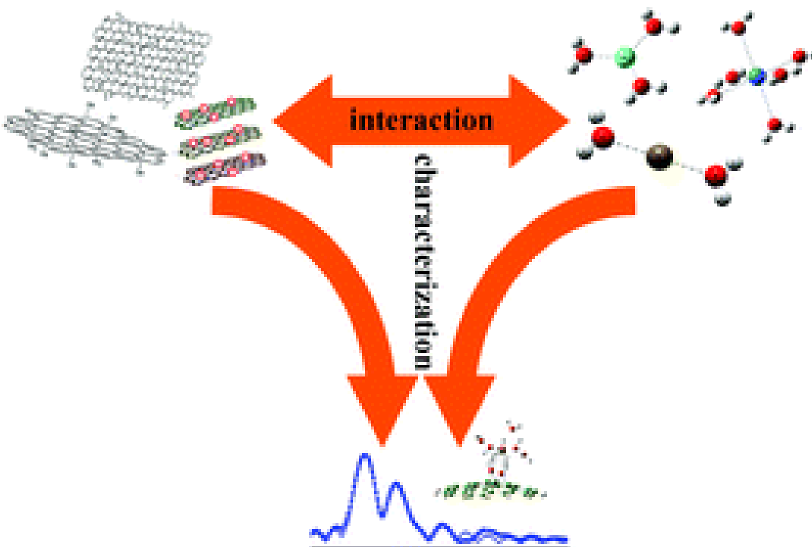

DISTINCTIVE NATIONAL NUCLEAR LABORATORY Sellafield Ltd NDA Nuclear Decommissioning Authority

Radionuclide immobilization

University of Strathclyde Engineering

In July 2016 synchrotron XRD measurements have been carried out on C-S-H samples.

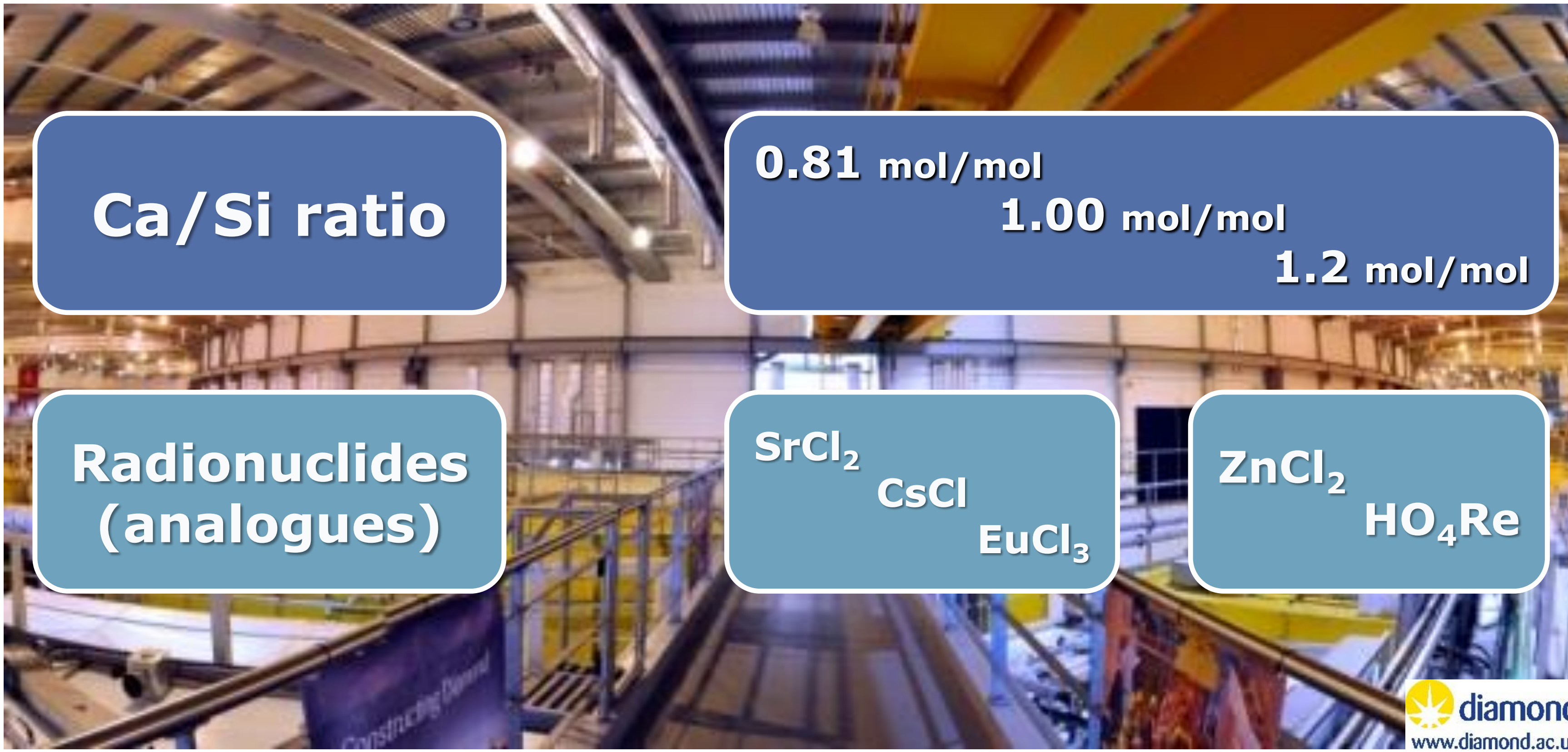

DISTINCTIVE

NATIONAL NUCLEAR LABORATORY

Sellafield Ltd

NDA Nuclear Decommissioning Authority

Radionuclide immobilization

In July 2016 synchrotron XRD measurements have been carried out on C-S-H samples.

Work in progress

Data analysis and interpretation

University of Strathclyde Engineering

INTRODUCTION

NANOPARTICLE CEMENT

C-S-H STRUCTURAL STUDY

RADIONUCLIDE IMMOBILIZATION

LOW PRESSURE NANOSILICA INJECTION

FUTURE WORK

DISTINCTIVE

NATIONAL NUCLEAR LABORATORY

Sellafield Ltd

NDA Nuclear Decommissioning Authority

Nanoparticle cement

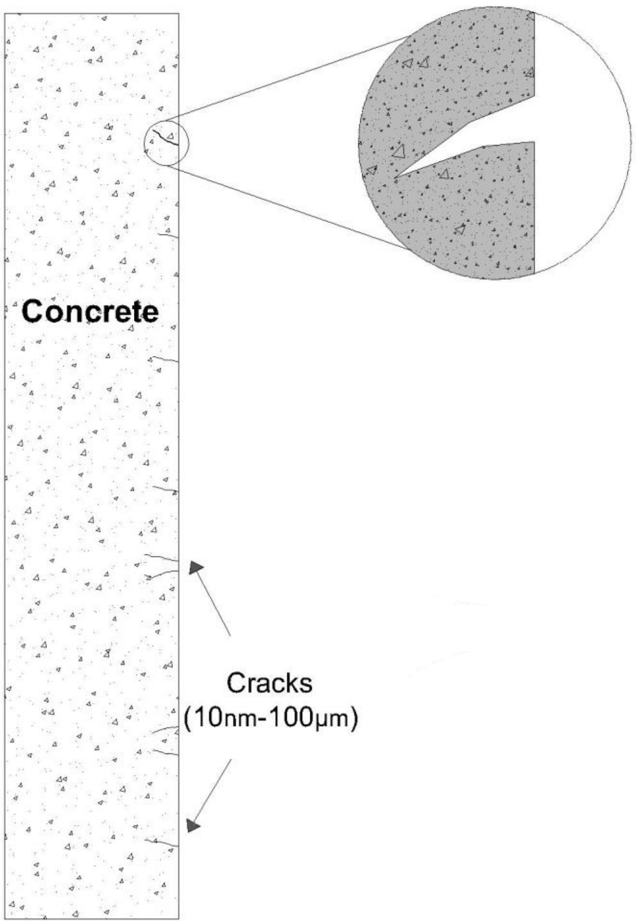

Aim of the project is to investigate new cement mixtures able to <u>seal</u> nano-cracks, <u>preventing</u> deterioration and giving and adequate (controlled) <u>impermeability</u> to existing concrete structures.

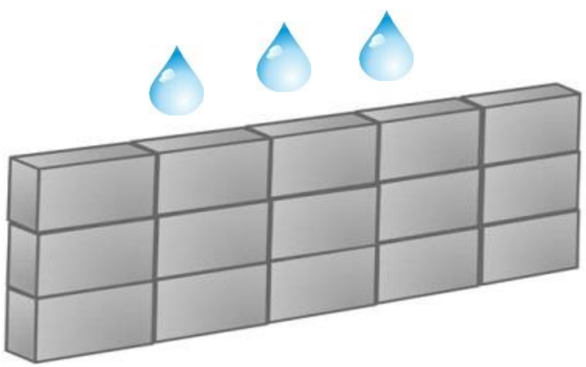

Nanoparticle cement

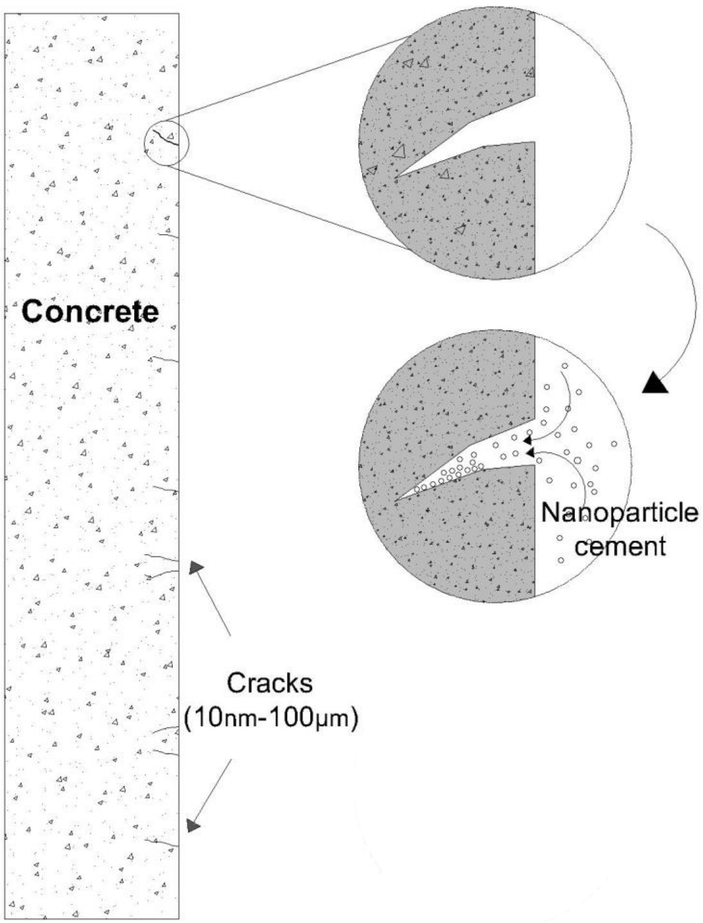

Aim of the project is to investigate new cement mixtures able to seal nano-cracks, preventing deterioration and giving and adequate (controlled) impermeability to existing concrete structures.

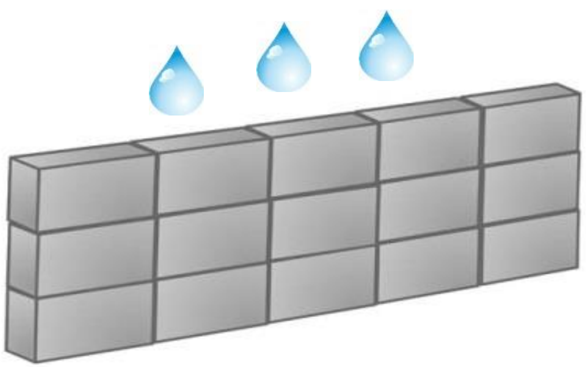

DISTINCTIVE NATIONAL NUCLEAR LABORATORY Sellafield Ltd NDA Nuclear Decommissioning Authority

Nanoparticle cement

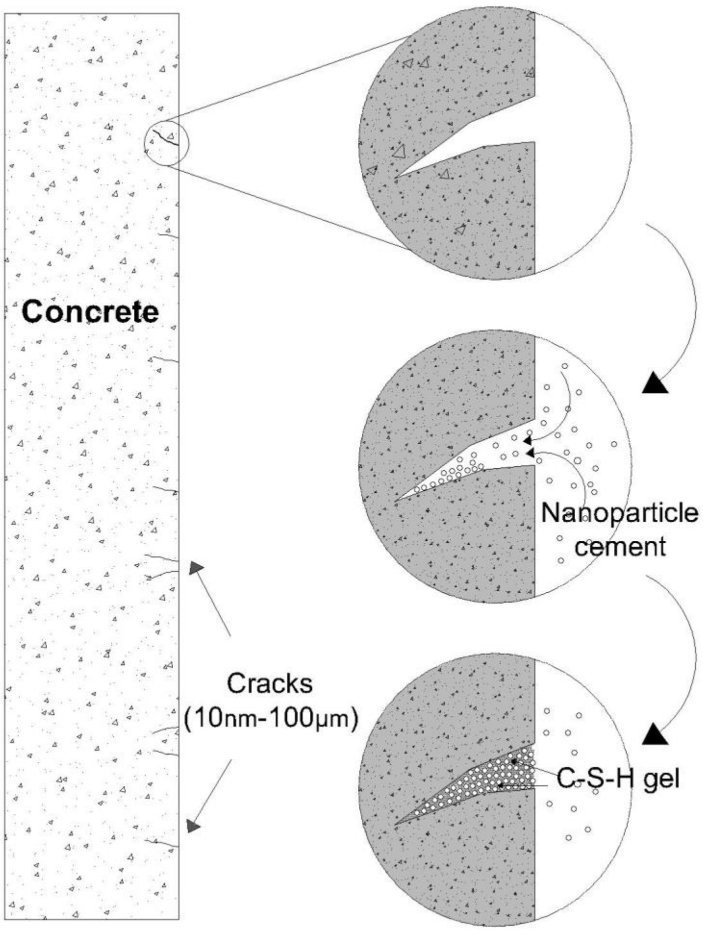

Aim of the project is to investigate new cement mixtures able to <u>seal</u> nano-cracks, <u>preventing</u> deterioration and giving and adequate (controlled) <u>impermeability</u> to existing concrete structures.

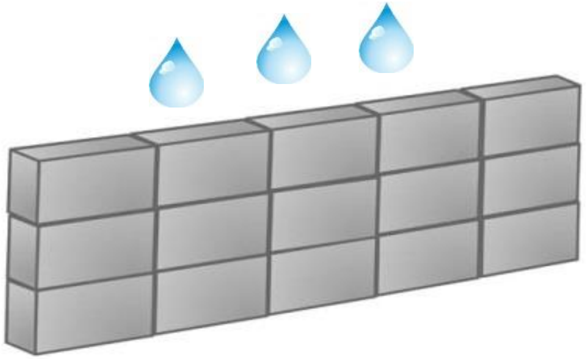

DISTINCTIVE

NATIONAL NUCLEAR LABORATORY

Sellafield Ltd

NDA Nuclear Decommissioning Authority

Materials

Portland cement

28 days curing

cement disc
h = 4mm
∅ = 35mm

Portland cement CEM II/A-L Strength class 42.5 MPa	
Components	%
Clinker	93
Gypsum added	7
Chemical composition (>0.2%)	
SiO_2	20.1
Al_2O_3	5.1
Fe_2O_3	3.4
CaO	63.0
MgO	2.6
SO_3	2.4
Na_2O	0.3
Density (g/cm^3)	3.2
Specific area (m^2/g)	0.38
Compressive strength, 28 days (MPa)	60

Nano-silica

Components	Nano-silica LUDOX T50©	Silica fume ELKEM©
State	Aqueous suspension	particles
Chemical composition (>0.2%)	%	%
SiO_2	50	99.9
Water	50	-
Particle size range (nm)	5-20	150-1000
Density (g/cm^3)	1.4	1.56
Specific area (m^2/g)	160	21.5

Silica fume

DISTINCTIVE NATIONAL NUCLEAR LABORATORY Sellafield Ltd NDA Nuclear Decommissioning Authority

Experimental set-up

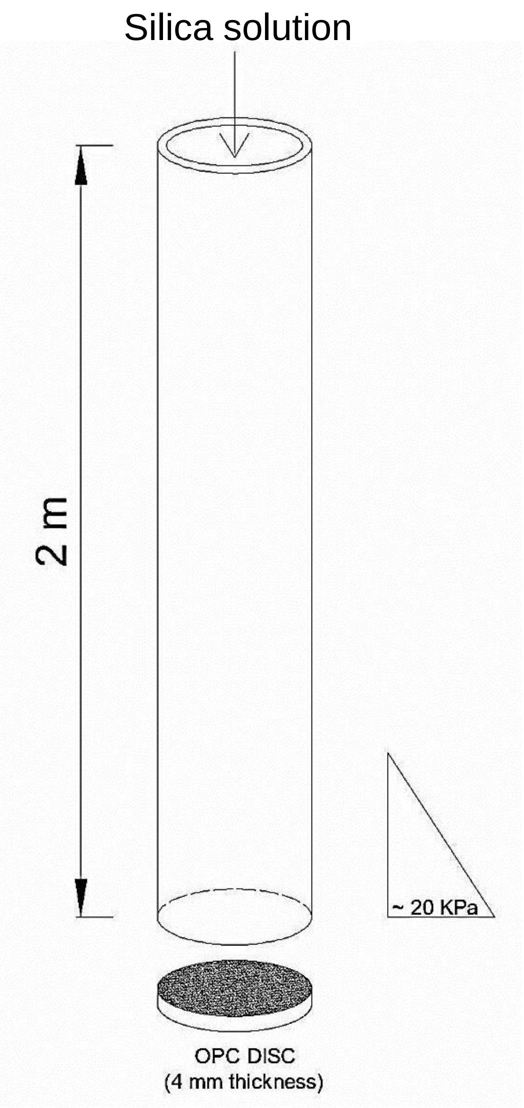

DISTINCTIVE

NATIONAL NUCLEAR LABORATORY

Sellafield Ltd

NDA Nuclear Decommissioning Authority

Experimental parameters

Particle size
of silica

Nano-silica (5-20 nm)

Silica fume (150-1000 nm)

Experimental parameters

University of Strathclyde Engineering

Particle size of silica	Nano-silica (5-20 nm) Silica fume (150-1000 nm)
Concentration of silica	10 % wt. 15 % wt. 20 % wt.

DISTINCTIVE

NATIONAL NUCLEAR LABORATORY

Sellafield Ltd

NDA Nuclear Decommissioning Authority

Experimental parameters

University of Strathclyde Engineering

Particle size of silica	Nano-silica (5-20 nm) Silica fume (150-1000 nm)
Concentration of silica	10 % wt. 15 % wt. 20 % wt.
Time of injection	7 days 14 days 28 day

Microstructural analysis

Silica particles will be forced to penetrate into *cement pores* in which an elevated **portlandite** content (naturally present in hydrated OPC as a result of hydration process) can be found. The particles will react with **calcium hydroxide** to form additional **C-S-H** and precipitate in the pores.

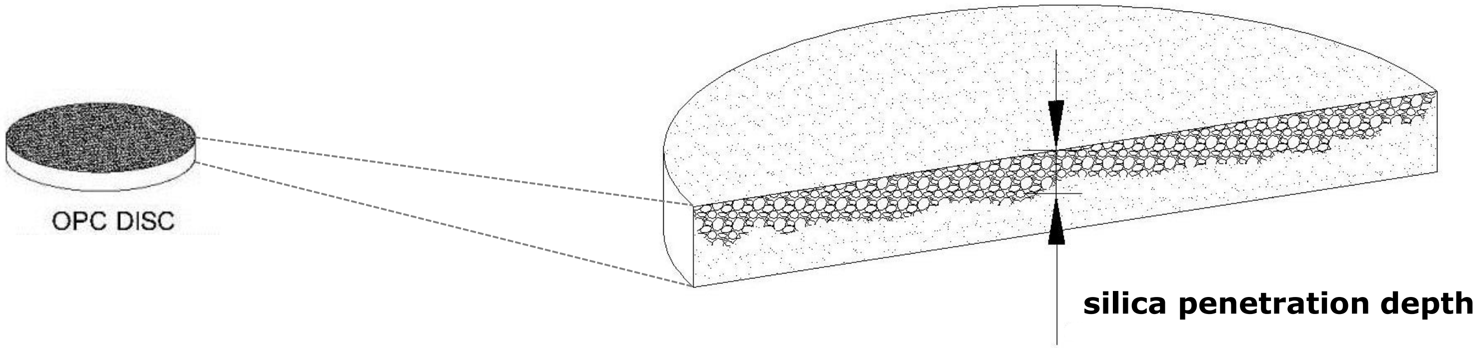

After injection OPC sample was characterised by:

- **Porosity** measurements and weight change
- Thermo-gravimetric analysis (**TGA**)
- Powder X-Ray diffraction (**XRD**)
- Scanning Electron Microscopy (**SEM)** imaging

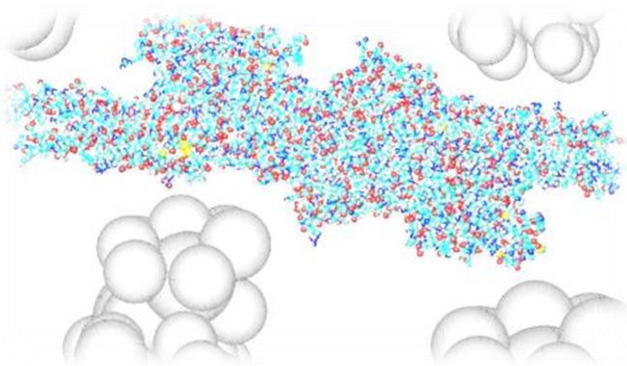

Weight change

At the end of the injection period, the disc was removed and oven-dried at 60 °C for ca. 100 hours. The sample weight was recorded before and after injection to quantify the amount of silica in the pores.

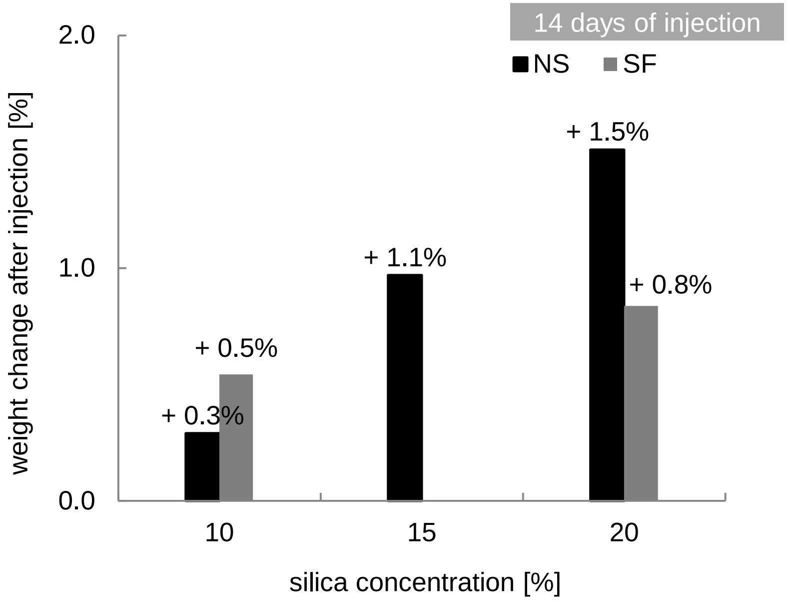

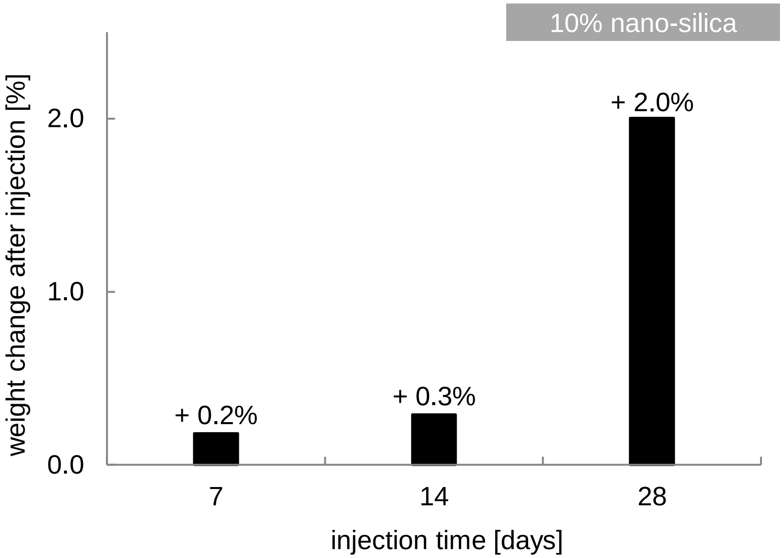

Porosity

Open porosity (***ψ***) was estimated by measuring the total water amount in each sample after oven-drying at 60 °C and overnight saturation in a vacuum chamber. Open porosity was calculated using the equation:

$$\psi = \frac{m_s - m_d}{V \cdot \rho}$$

where $\boldsymbol{\psi}$ is the open porosity, $\boldsymbol{m_s}$ is the sample water saturated mass (kg), $\boldsymbol{m_d}$ is the sample dried mass (kg), $\boldsymbol{V}$ is the volume of the sample (m^3) and $\boldsymbol{\rho}$ is the density of the water at 20 °C (kg/m^3).

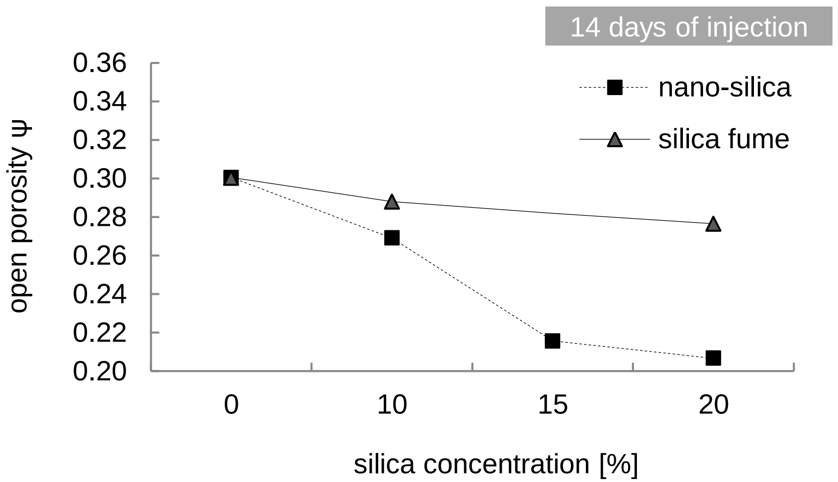

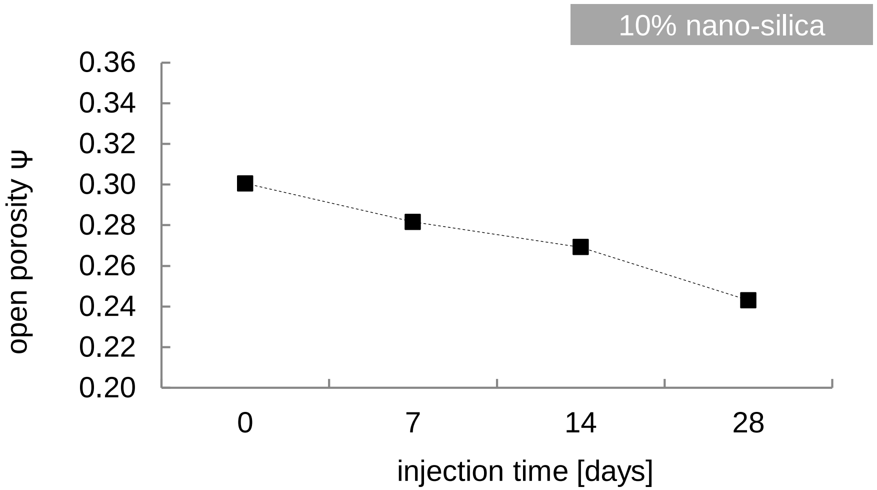

Thermogravimetric analysis

An average of 20 mg was sampled from the cross section of the disc and powdered. Thermal analyses were conducted at a heating rate of 10 °C min^{-1} from 25 °C to 1000 °C under nitrogen gas flow, using a Netzsch simultaneous analyzer.

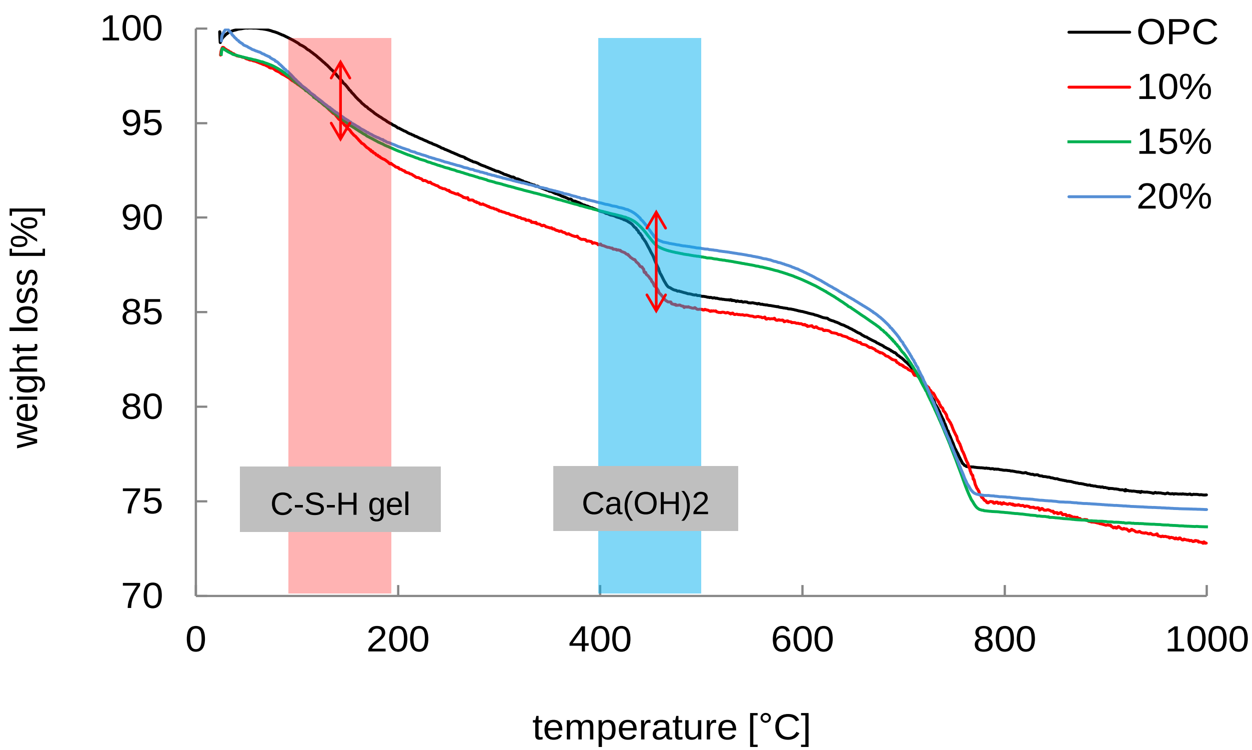

DISTINCTIVE

NATIONAL NUCLEAR LABORATORY

Sellafield Ltd

NDA Nuclear Decommissioning Authority

Thermogravimetric analysis

The relative content of **C-S-H** gel and portlandite **$Ca(OH)_2$** at different nano-silica concentrations values.

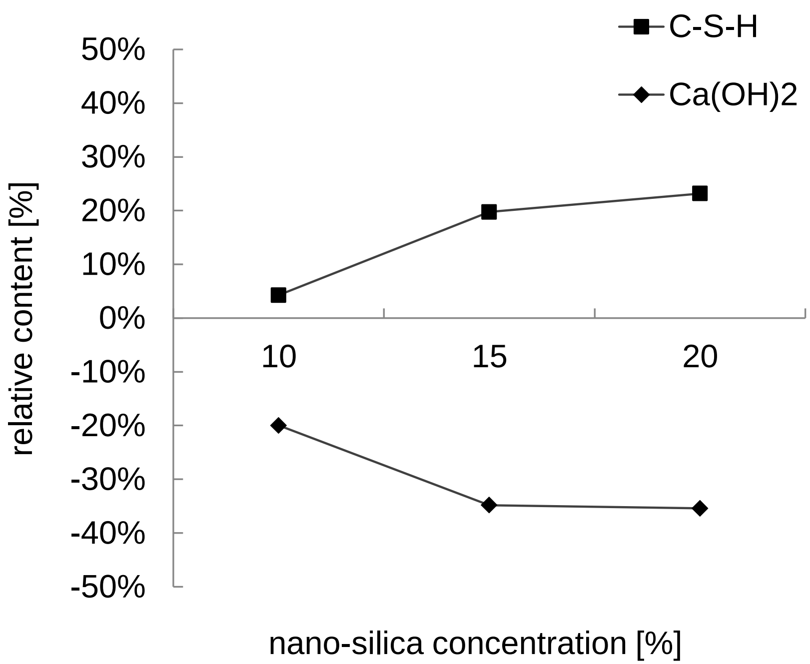

After 14 days of injection

Thermogravimetric analysis

The relative content of **C-S-H** gel and portlandite **$Ca(OH)_2$** at different nano-silica concentrations values.

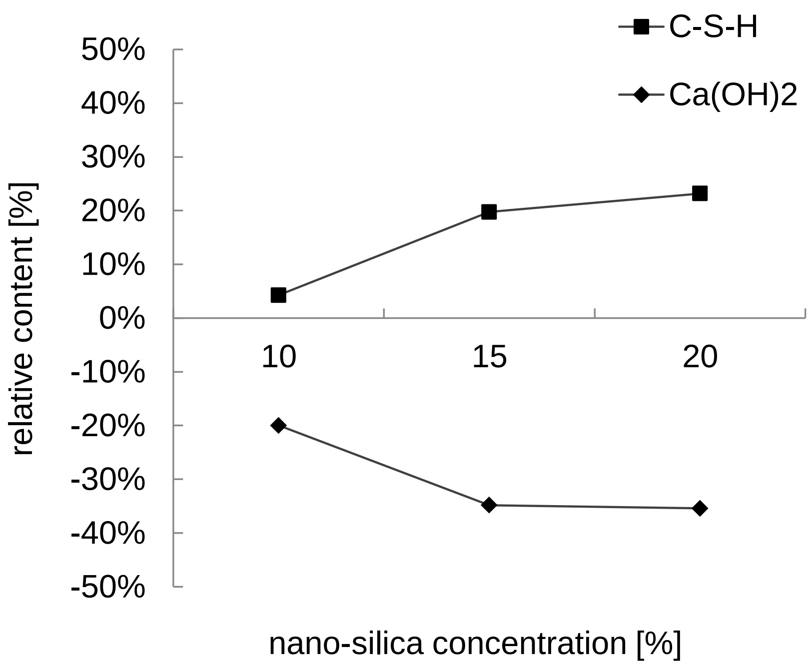

The relative content of portlandite in respect to the silica concentration:

nano-silica Vs silica fume

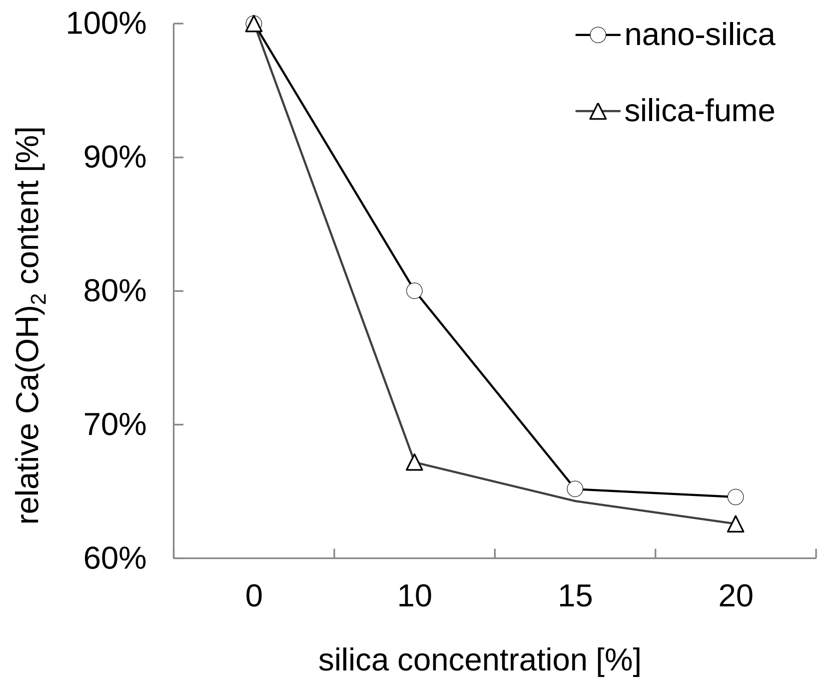

After 14 days of injection

SEM imaging

The silica concentration (10%, 15% and 20% wt.) influences the penetration depth, at a fixed injection time (14 days)

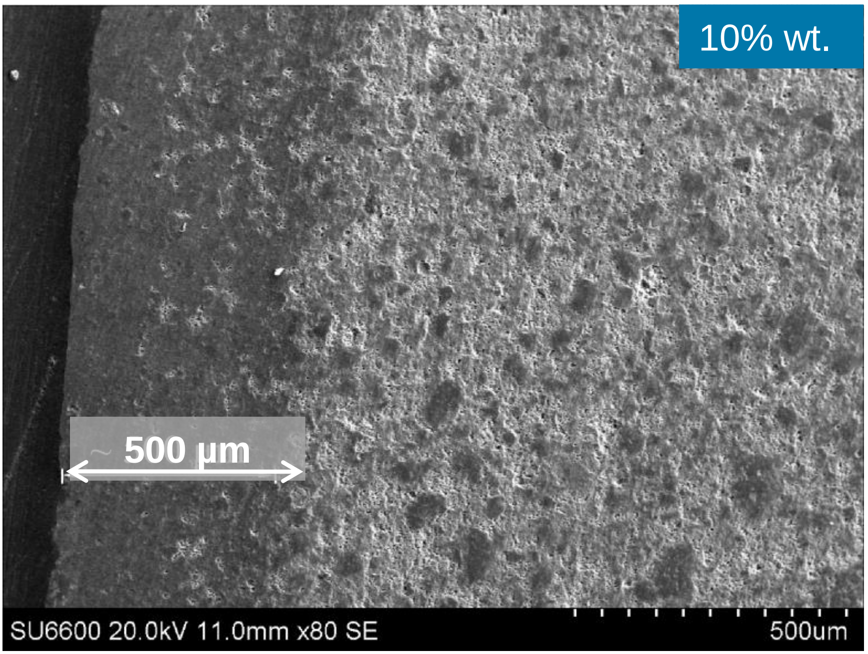

nano-silica injection

After 14 days of injection

DISTINCTIVE

NATIONAL NUCLEAR LABORATORY

Sellafield Ltd

NDA Nuclear Decommissioning Authority

SEM imaging

University of Strathclyde Engineering

The silica concentration (10%, 15% and 20% wt.) influences the penetration depth, at a fixed injection time (14 days)

nano-silica injection

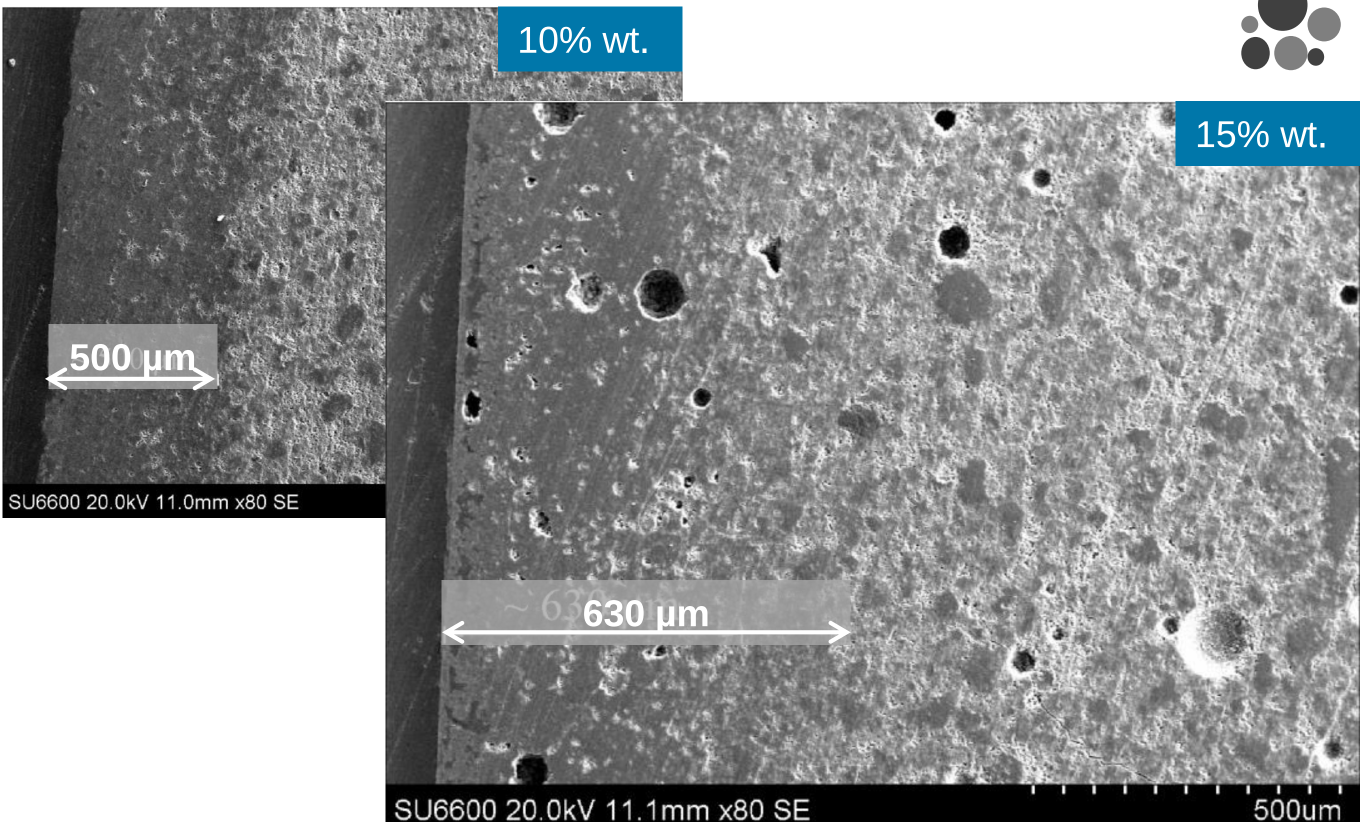

DISTINCTIVE

NATIONAL NUCLEAR LABORATORY

Sellafield Ltd

NDA Nuclear Decommissioning Authority

SEM imaging

University of Strathclyde Engineering

The silica concentration (10%, 15% and 20% wt.) influences the penetration depth, at a fixed injection time (14 days)

nano-silica injection

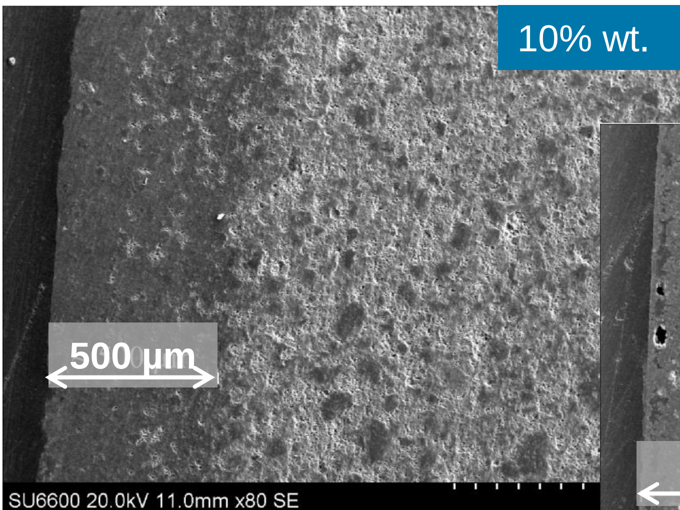

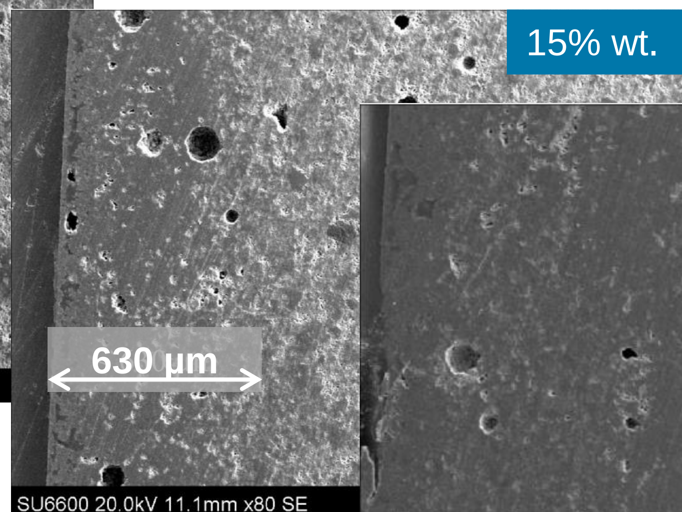

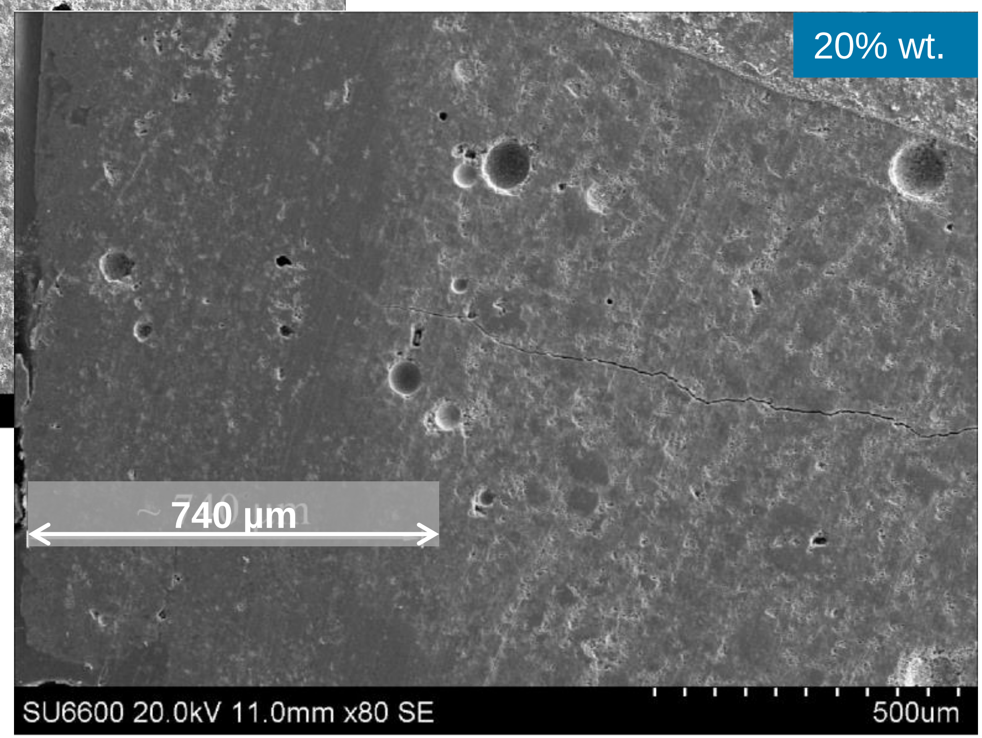

After 14 days of injection

DISTINCTIVE

NATIONAL NUCLEAR LABORATORY

Conclusions

1. Low-pressure (20 kPa) silica injection has effectively impregnated cement samples. After 14 days of injection with a nano-silica suspension of 20% wt. concentration, we observed a total reduction of 30% in porosity, suggesting this is a potential consolidant for friable or cracked concrete.

Particle size
of silica

Nano-silica (5-20 nm)

Conclusions

1. Low-pressure (20 kPa) silica injection has effectively impregnated cement samples. After 14 days of injection with a nano-silica suspension of 20% wt. concentration, we observed a total reduction of 30% in porosity, suggesting this is a potential consolidant for friable or cracked concrete.

Particle size of silica	**Nano-silica (5-20 nm)**
Concentration of silica	**20 % wt.**

Conclusions

University of Strathclyde Engineering

1. Low-pressure (20 kPa) silica injection has effectively impregnated cement samples. After 14 days of injection with a nano-silica suspension of 20% wt. concentration, we observed a total reduction of 30% in porosity, suggesting this is a potential consolidant for friable or cracked concrete.

Particle size of silica	**Nano-silica (5-20 nm)**
Concentration of silica	**20 % wt.**
Time of injection	**14 days**

DISTINCTIVE

NATIONAL NUCLEAR LABORATORY

Sellafield Ltd

NDA Nuclear Decommissioning Authority

Conclusions

2. After 14 days of nano-silica injection an average penetration depth of ca. 745 µm of was measured, which is ca. 20% of the cross section of the sample (4 mm).

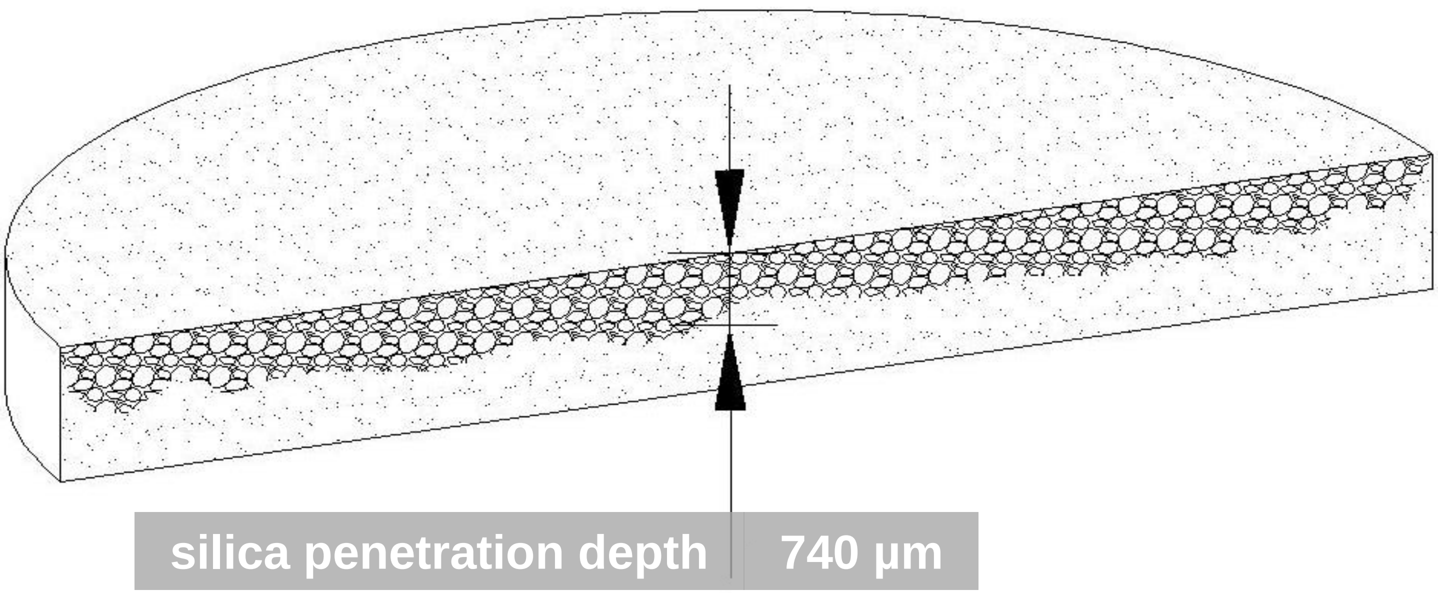

After 14 days of injection

DISTINCTIVE

NATIONAL NUCLEAR LABORATORY

Sellafield Ltd

NDA Nuclear Decommissioning Authority

Research output

Research article

Low-pressure silica injection for porosity reduction in cementitious materials

In press: **Journal of Construction and Building Materials**
Editor: Elsevier Inc.
Date: November 2016

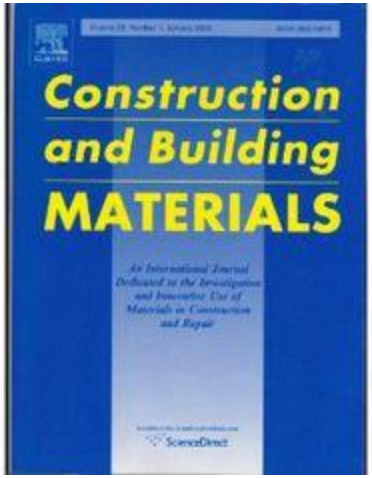

Conclusions

1. **Nanoparticles in cement show a higher reactivity compared to traditional OPC.**
2. **C-S-H synthesis** methods and different calcium sources affect the formation of C-S-H and structural changes have been observed.
3. C-S-H structure can be altered and tailored in order to ***house*** other atoms.
4. **Immobilisation** of radionuclides into C-S-H phase can occur through different mechanism: from structural incorporation to surface interaction.
5. Injection of nanosilica promotes *decrease of porosity* and formation of **additional C-S-H**. Controlling the C/S ratio and other parameters, this additional C-S-H could be tailored in order to immobilise radionuclides and precipitate into nano-cracks.

DISTINCTIVE NATIONAL NUCLEAR LABORATORY Sellafield Ltd NDA Nuclear Decommissioning Authority

Future work

1. **Synchrotron XRD** *data analysis will give a further insight into the interaction mechanism between C-S-H phase and radionuclides.*

2. ***^{29}Si NMR spectroscopy*** *measurements will be carried out on C-S-H gel and radionuclides, in order to investigate the immobilisation capability and structural information. The analysis will be carried out at the Department of Civil Engineering of* ***Tsinghua University in Beijing*** *(CHINA), supported by G.R.E.A.T. project.*

Workflow chart

University of Strathclyde Engineering

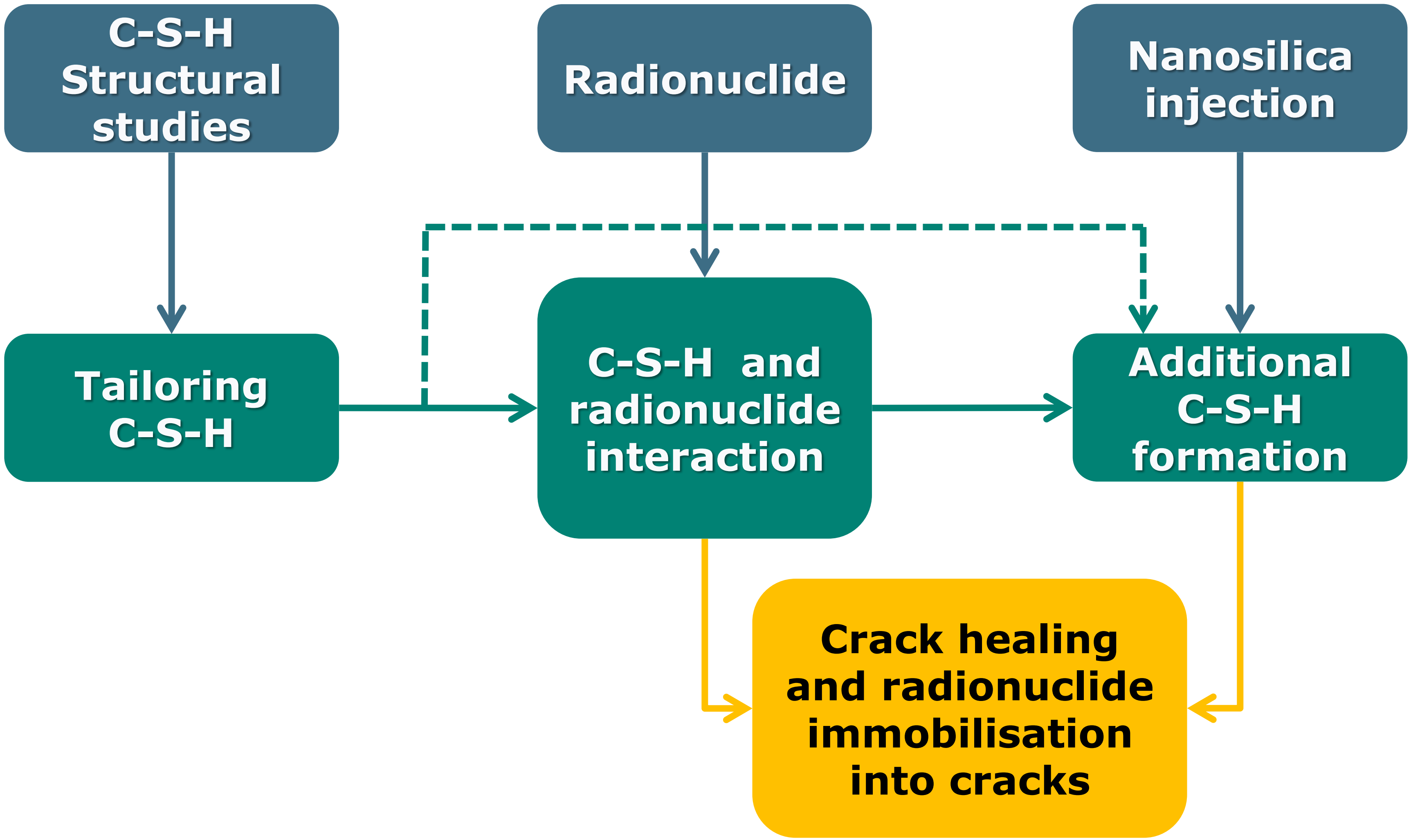

DISTINCTIVE

NATIONAL NUCLEAR LABORATORY

Sellafield Ltd

NDA Nuclear Decommissioning Authority

University of Strathclyde
Engineering

Riccardo Maddalena

University of Strathclyde, Glasgow - UK

DISTINCTIVE

NATIONAL NUCLEAR LABORATORY

Sellafield Ltd

NDA Nuclear Decommissioning Authority

Nanoparticle injection

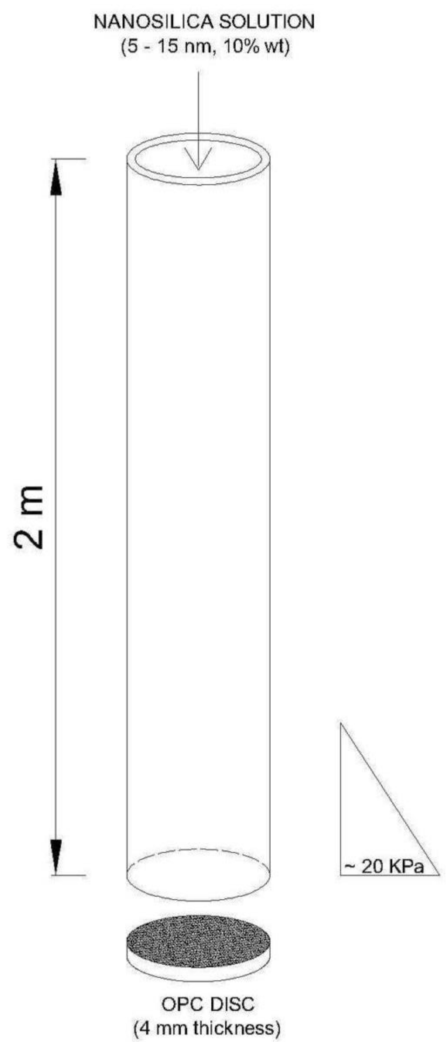

Low-pressure nanosilica injection was investigated at lab-scale. A solution of **nanosilica** (particle size range of 5 – 15 nm) will be injected through a *28 days cured OPC* disc (thickness 4 mm) at a ~ **20 kPa** of hydrostatic pressure.

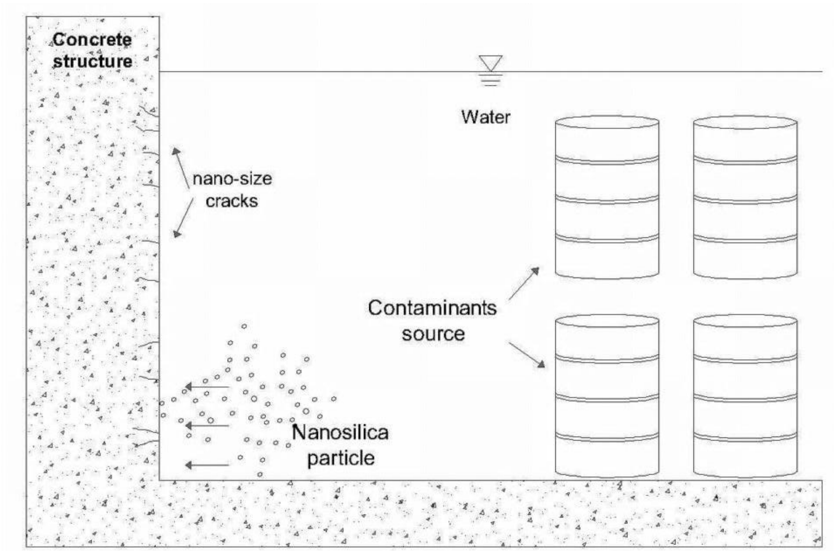

Application of low-pressure injection in legacy ponds concrete structures

Actinide interactions with waste and structural materials

Pieter Bots

K. Morris, R. Hibberd, G.T.W. Law, J.F.W. Mosselmans, A. Brown, J. Doutch, A. Smith, T.A. Marshall, A. van Veelen, C. Muryn, R. Wogelius and S. Shaw

Outline

- Introduction
- Np(V) fate during iron oxide crystallization
- Actinide interaction with magnetite(111) surfaces
- Summary

Geological disposal of radioactive waste

Waste management via disposal in Geological Disposal Facilities preferred option.

UK: Cement in GDF creates a hyperalkaline (pH > 9) groundwater plume

Corrosion of metals in construction and waste materials

Affect the (geo)chemistry of many actinides of concern

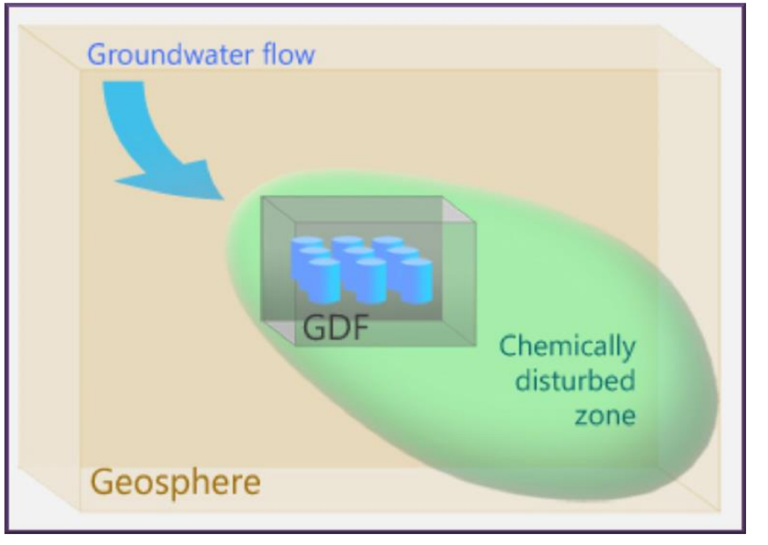

http://dev.bigradnerc.com/project-information/

Uranium, most dominant by mass
Neptunium, a major dose contributing radionuclide
Plutonium, major product in nuclear fuel cycle

Rationale

Understanding actinide geochemistry and behaviour is important

Focus on interaction with iron oxides

Relevant to waste management scenarios

Geochemistry of U, Np and Pu under these conditions is not well understood

- Speciation
- Sorption
- Incorporation
- Redox

Np(V) interaction during Fe(III)-(oxyhydr)oxide crystallization

Adsorption of Np(V) to Ferrihydrite at pH 9.5 and 11

Crystallisation of ferrihydrite to hematite (Fe_2O_3) or goethite (FeOOH)

- In the presence and absence of Np(V)

Analyses

- XRD
- Acid leach + ICP-MS
- First ever Np XAS analyses at Diamond Light Source

Experiment	pH	Temp (°C)	Scope
Hcont	10.5	120	Fate of Np during the crystallisation of ferrihydrite to hematite
Gcont	13.3	RT	Fate of Np during the crystallisation of ferrihydrite to goethite

Np(V) during ferrihydrite crystallisation

XRD and TEM confirm the formation of only hematite and goethite

Acid leach and shift in features in XANES spectra indicate

Hematite

- Np(V) incorporated

Goethite

- Acid leachable Np(V) phase

Sample name	%Np pre-leach	%Np post-leach
Hematite	100(0)	94(0)
Goethite	100(0)	22(3)

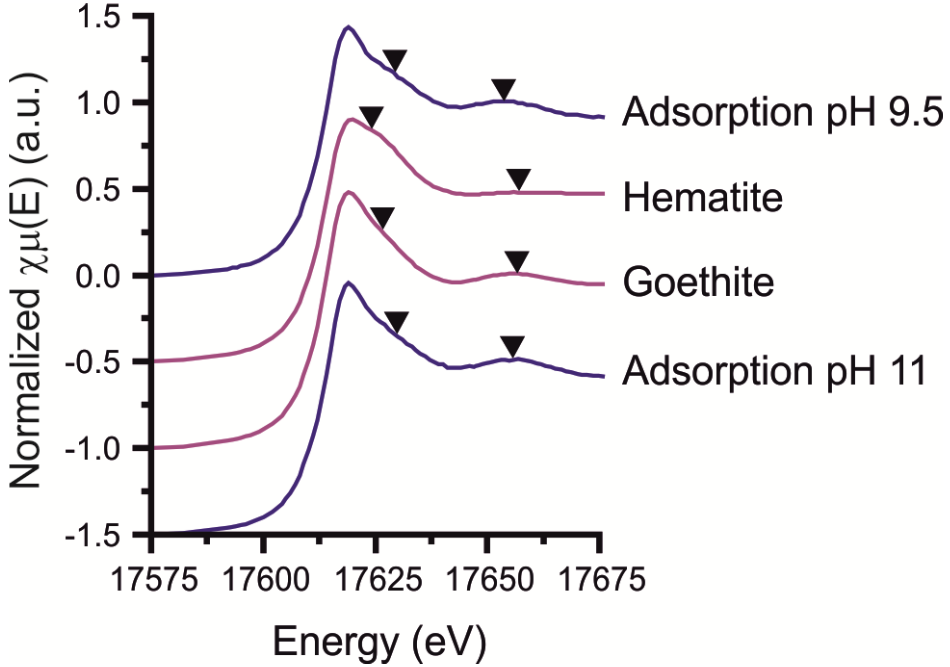

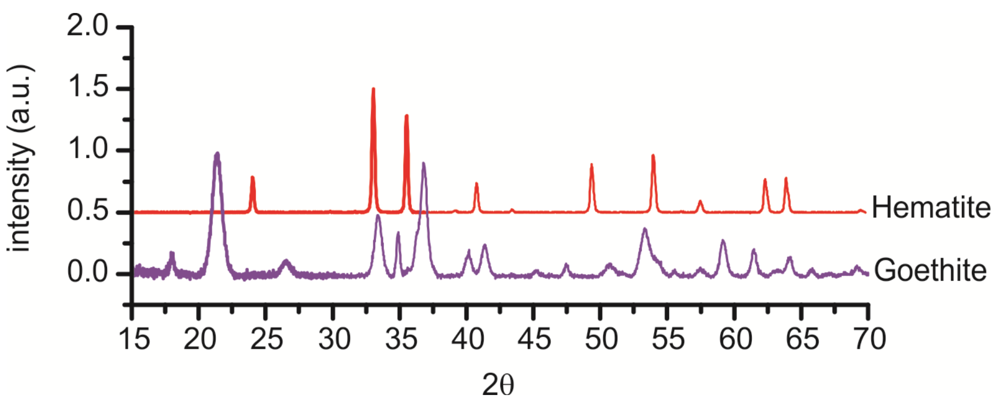

Np(V) incorporation in hematite

8% Np(V) release into solution after acid leach

6-fold coordinated Np(V)

- loss of dioxogenyl NpO_2^+ suggesting distortion

Np-Fe bonds consistent with direct substitution for octahedral iron in the structure of hematite

Path	CN	R (Å)	σ^2 (Å²)	Hematite (CIF) CN	R (Å)	ΔR (%)
$Np\text{-}O_{ax}$	1	1.86(1)	0.0014(4)			
$Np\text{-}O_{eq}$	2	2.16(1)	0.007(1)	3	1.95	11
$Np\text{-}O_{eq}$	3	2.39(2)	0.007*	3	2.12	13
Np-Fe	1	2.97(2)	0.011(1)	1	2.90	1
Np-Fe	3	3.11(1)	0.011*	3	2.97	5
Np-Fe	3	3.37(2)	0.011*	3	3.36	0.3
Np-Fe	3	3.56(2)	0.011*	6	3.71	-4

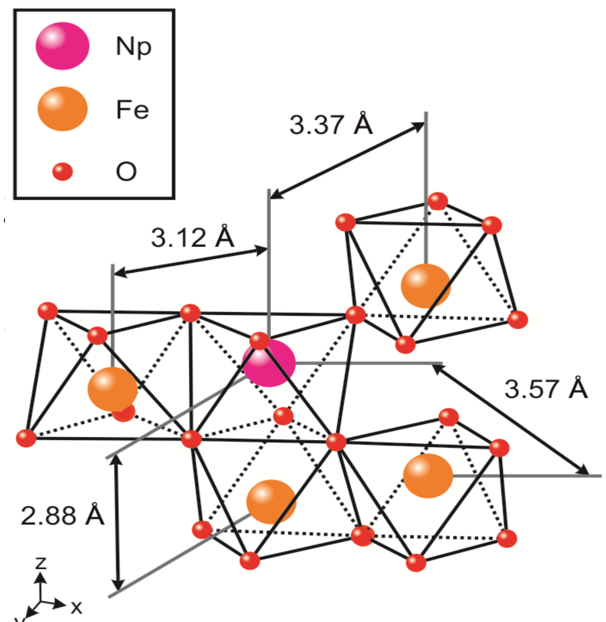

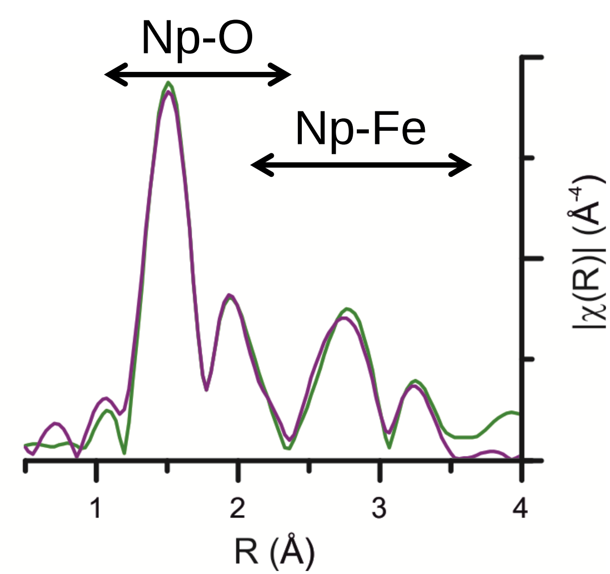

Np(V) behaviour during goethite crystallisation

MANCHESTER 1824
The University of Manchester

University of Strathclyde Engineering

- Acid leach released 78 % into solution
- EXAFS very similar as NpO_2OH (Gaona et al. 2012 and 2013)

Possible phases

- $NpO_2(OH)$ (undersaturated)
- $Ca_{0.5}NpO_2(OH)_2$ (supersaturated)
- $NaNpO_2(OH)_2$ (no data)

Sample	Path	CN	R (Å)	σ^2 (Å^2)	NpO_2OH (EXAFS) CN	R (Å)
	$Np\text{-}O_{ax}$	2	1.88(1)	0.004(1)	2	1.86
	$Np\text{-}O_{eq}$	1.5	2.25(2)	0.005(2)	2	2.23
	$Np\text{-}O_{eq}$	3.5	2.43(2)	0.005*	3	2.42

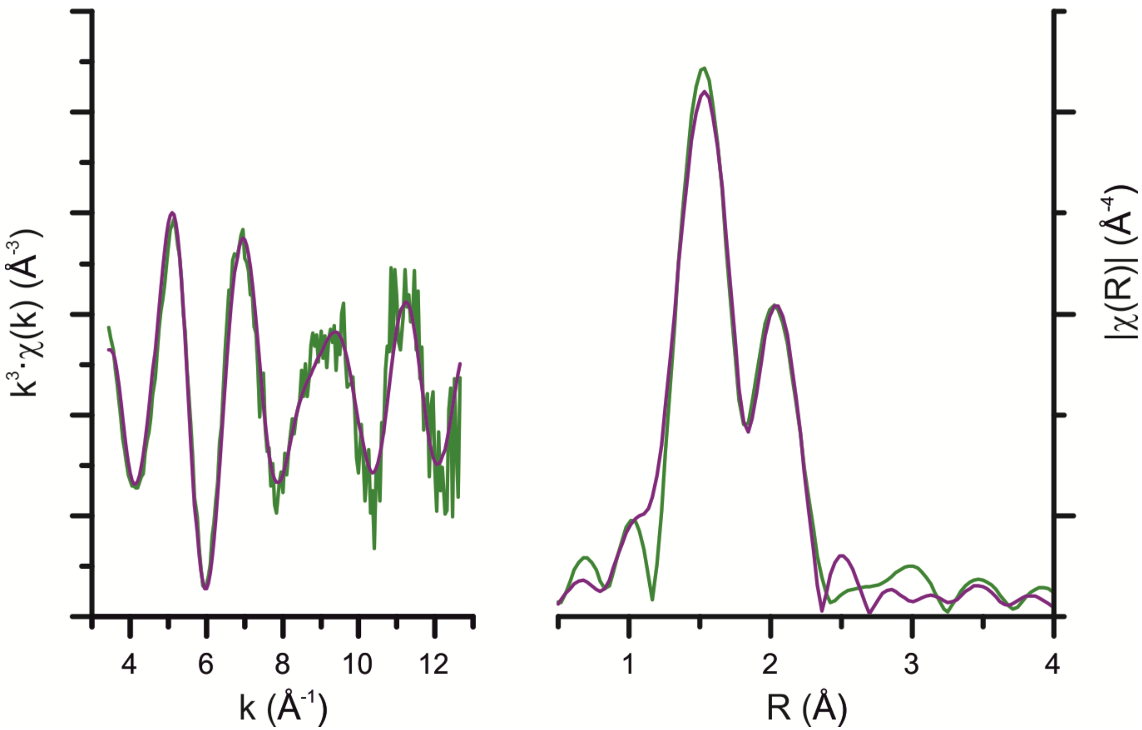

Conclusions

1. Np(V) directly replaces 6-fold coordinated Fe(III) in the crystalline structure of hematite (pH 10.5)
2. Forms a disordered neptunyl hydroxide / neptunate solid at pH 13.3

(Bots et al. 2016 – *Environmental Science and Technology*)

MANCHESTER
1824
The University of Manchester

WILLIAMSON
RESEARCH CENTRE
for Molecular Environmental Science

University of
Strathclyde
Engineering

CRR
Centre for
Radiochemistry Research

KIT
Karlsruher Institut für Technologie

BIogeochemical Gradients
and RADionuclide transport
BIGRAD
www.bigradnerc.com

ANKA

diamond

Re-use and Volume Reduction of Scabbled Contaminated Concrete

Toby Lord Dr Leon Black

Overview

- Introduction & Background
  - Contaminated concrete
  - Scabbling
  - Research basis
- Cementitious replacement
  - Characterisation
  - Replacement
- Ternary grout
- LIBS for contamination detection

Contaminated Concrete

- Contamination through direct contact with radionuclide containing air or water.
- Radionuclides can be physically or chemically bonded to the concrete[1];
  - soluble elements within pore water, physically bonded.
  - chemical bonding onto different phases within cement matrix or gel.
- Also products from activation of concrete and reinforcing steel exposed to neutron flux.
- Depth of contamination depends on radionuclide. ^{239}I shown to penetrate up to several cm in degraded concrete, but more particulate Pu remains on surface.
- Radionuclides expected depend on exposure history of concrete.

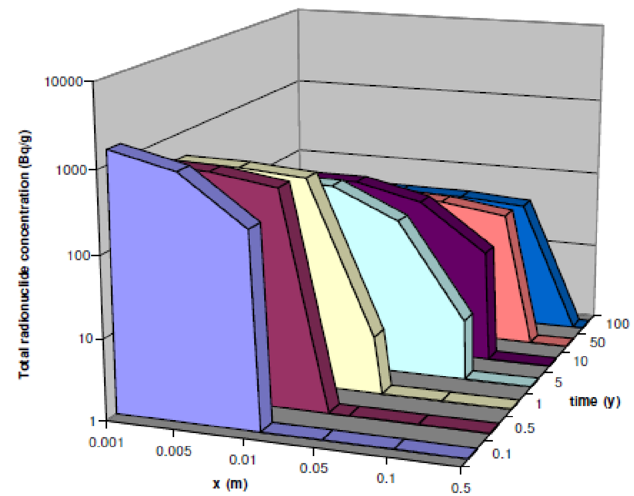

Figure 1. In-diffusion of contamination from the surface of a concrete slab (at the left side of the plot) after periods from 0.1 to 100 years. $D_e = 10^{-11}$ m^2/s, $K_d = 1$ (e.g. ^{129}I), $\varepsilon = 0.25$.

[1] BATH, A., DEISSMANN, G. & JEFFERIS, S. 2003. Radioactive Contamination of Concrete: Uptake and Release of Radionuclides. *The 9th International Conference on Radioactive Waste Management and Environmental Remediation.* Oxford: ICEM.

Scabbled Concrete

- Removal of outer contaminated layer from bulk concrete.
- Physical or mechanical removal – laser, microwave, grinding, water blasting, liquid nitrogen.
- Intact bulk concrete remains, particulate scabblings removed for treatment.
- Enables bulk concrete to be disposed of as VLLW or exempt waste.
- Arising scabblings currently treated as LLW or mostly ILW, requiring disposal.

Research Basis

- Over 50% UK's nuclear waste is concrete and building rubble and over 2,000,000 tonnes of concrete at Sellafield site alone.
- During decommissioning large volumes of contaminated scabbled concrete will arise requiring disposal. 2013 waste inventory shows 59,000 tonnes concrete, sand and rubble conditioned or from future arising's[3].
- With very high disposal costs of £14,000 per m^3 of ILW[2], this will prove very costly.
- As part of Waste Management Hierarchy, re-use and volume reduction of waste is preferable to disposal – co-disposal within grout matrix encapsulating other waste.

[2] DEPARTMENT OF ENERGY & CLIMATE CHANGE 2011. Waste Transfer Pricing Methodology for the Disposal of Higher Activity Waste from Nuclear Power Stations. London: Department of Energy and Climate Change.
[3] PÖYRY ENERGY LIMITED & AMEC PLC 2014. The 2013 UK Radioactive Waste Inventory. Moor Row, Cumbria.

UNIVERSITY OF LEEDS

Characterisation

- Scabbled material is fine, particulate material
  - Particle size – two dominant materials, non-uniform size distribution

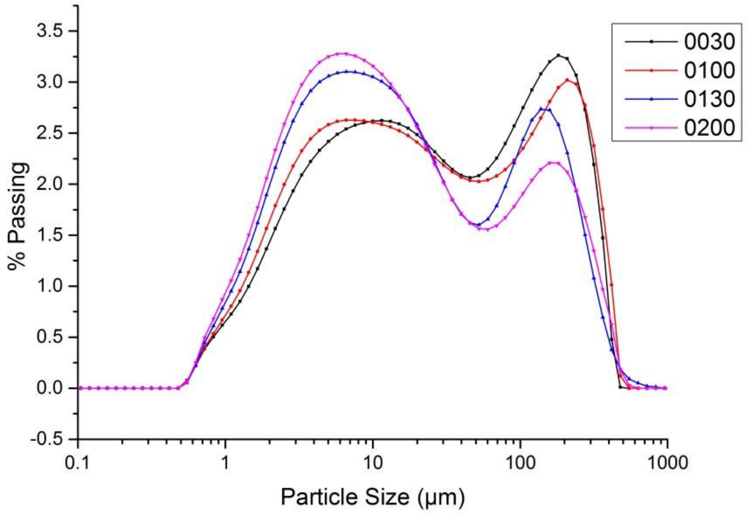

  - Particle shape – dominated by high energy scabbling processes
- Is there any remaining reactivity?
  - XRD, TGA analysis - presence of anhydrous material
  - Calorimetry – increased heat of hydration

Cementitious Replacement

- Use of scabbled material as a binder replacement within encapsulation grouts – co-disposal.
- Stringent specifications
  - Heat output - cumulative heat of hydration must be less than 250 Joules per gram within the first 24 hours after casting.
  - Fluidity – Colflow testing
  - Setting time – between 4 and 24 hours
  - Bleed – less than 1% by mass
  - BFS:OPC ratio to be 3:1
- At what replacement level will grout still meet specifications?
- 10, 20 and 40% replacement levels to be used within a number of tests

- Heat output measured through calorimetry – quartz used as inert reference
- Fluidity measured using Colflow test requiring two pints of grout
  - Due to large volumes, and limited synthesised material, desktop rheometry required – link between colflow and desktop rheometry being investigated.
  - Envelope of grout viscosity in which Colflow test will be passed
- Setting time and bleed measured through standard industry testing
- Replacement of total binder content to be carried out – replacing individual components creates too many variables.

Ternary Grouts

- Ternary cements are those with high CRM levels, as well as the addition of limestone or calcium carbonate.
- Scabbling to occur on outer surfaces of aged concrete structures – carbonation of cement paste very likely to have occurred, in which case calcium carbonate is present.
- Behaviour of high BFS grout with inclusion of calcium carbonate from recycled scabblings to be investigated.

- Stabilisation of AFt phases can lead to densification of cement matrix – reduced porosity and permeability could be advantageous for long term durability.
- Similar experimental procedure to cementitious replacement, but shift of focus onto effect of carbonated material on properties of grout. Accelerated carbonation of synthesised material will take place.
- Early age heat output may increase – could limit maximum replacement level.
- Plans to investigate changes in porosity and permeability using X-CT at central lab.

LIBS for Contamination Detection

Laser Induced Breakdown Spectroscopy

- High powered laser creates plasma on surface of sample
- Light spectroscopy carried out on plasma
- Results produced on wavelength and intensity plot – elements have known wavelengths
- 6 samples made with either standard cement or 20% PFA replacement
- 2 control samples, 2 with 1 wt% contaminants, 2 with 0.1 wt% contaminants
- Copper sulphate, potassium iodide and cerium oxide used

- Initially laser intensity kept below detector saturation point for all elements, and no differences observed.
- Intensity then increased such that saturation occurred for some elements, but amplified the peaks of other trace constituents, including contaminants

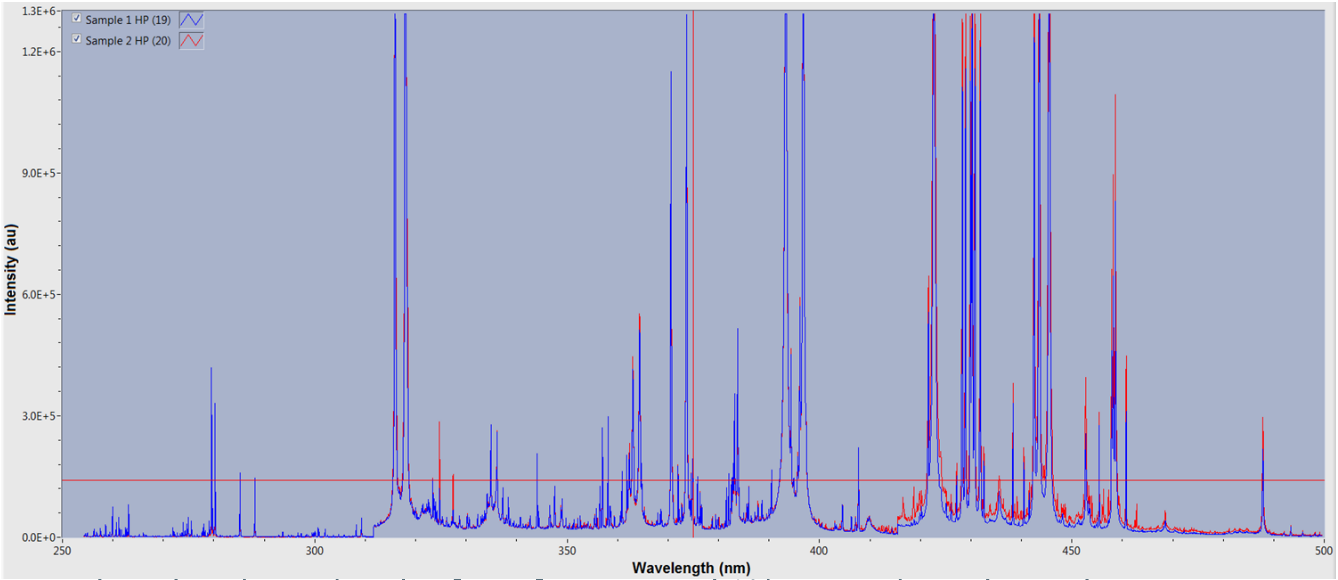

wavelength vs intensity plot for reference and 1% contaminated sample

- When laser intensity increased, visible peaks attained for contaminants
- Two known copper wavelengths, 324.7540 and 327.3957, showing clear increased intensity for samples with copper sulphate addition

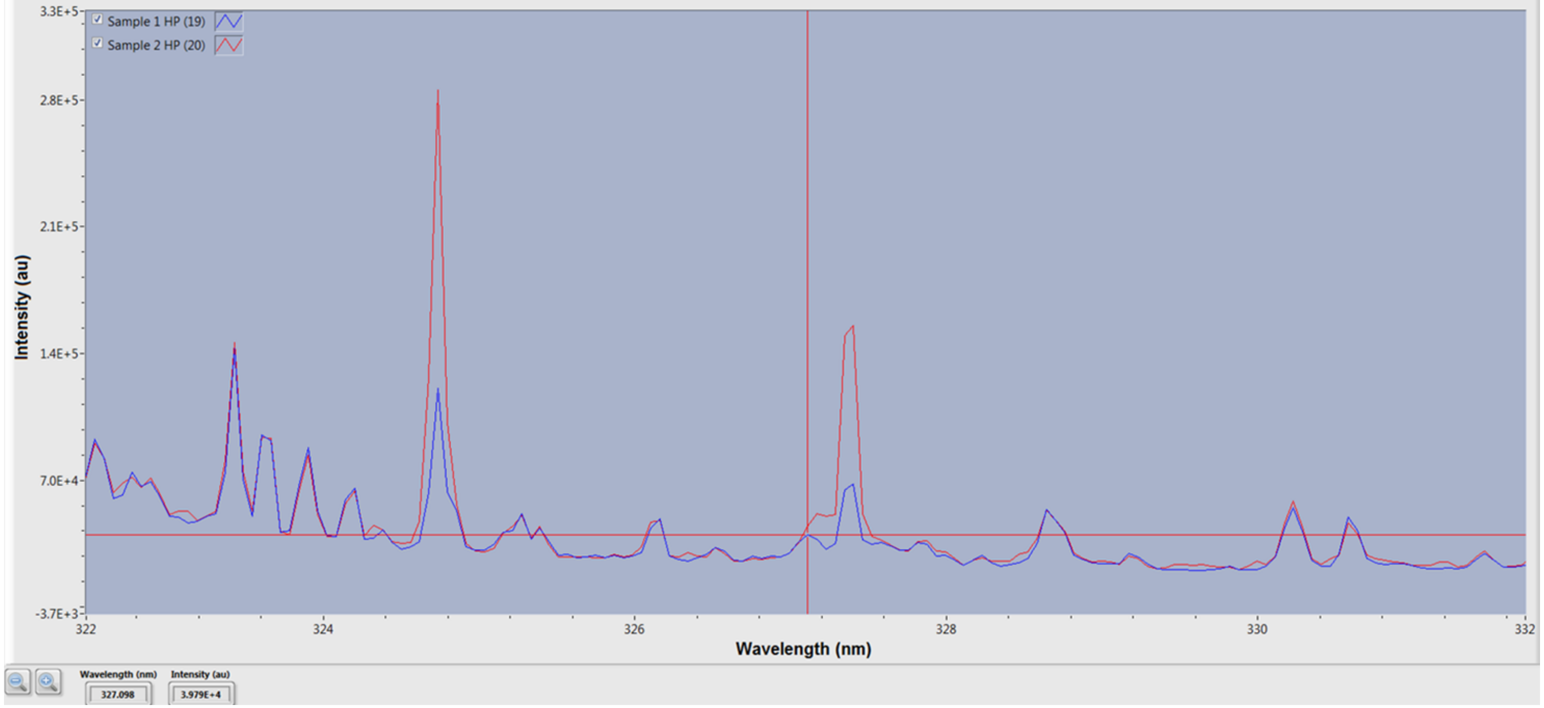

UNIVERSITY OF LEEDS

- When laser intensity increased, visible peaks attained for contaminants
- Peaks for cerium also identified, including very slights peaks for 0.1 wt% contaminants

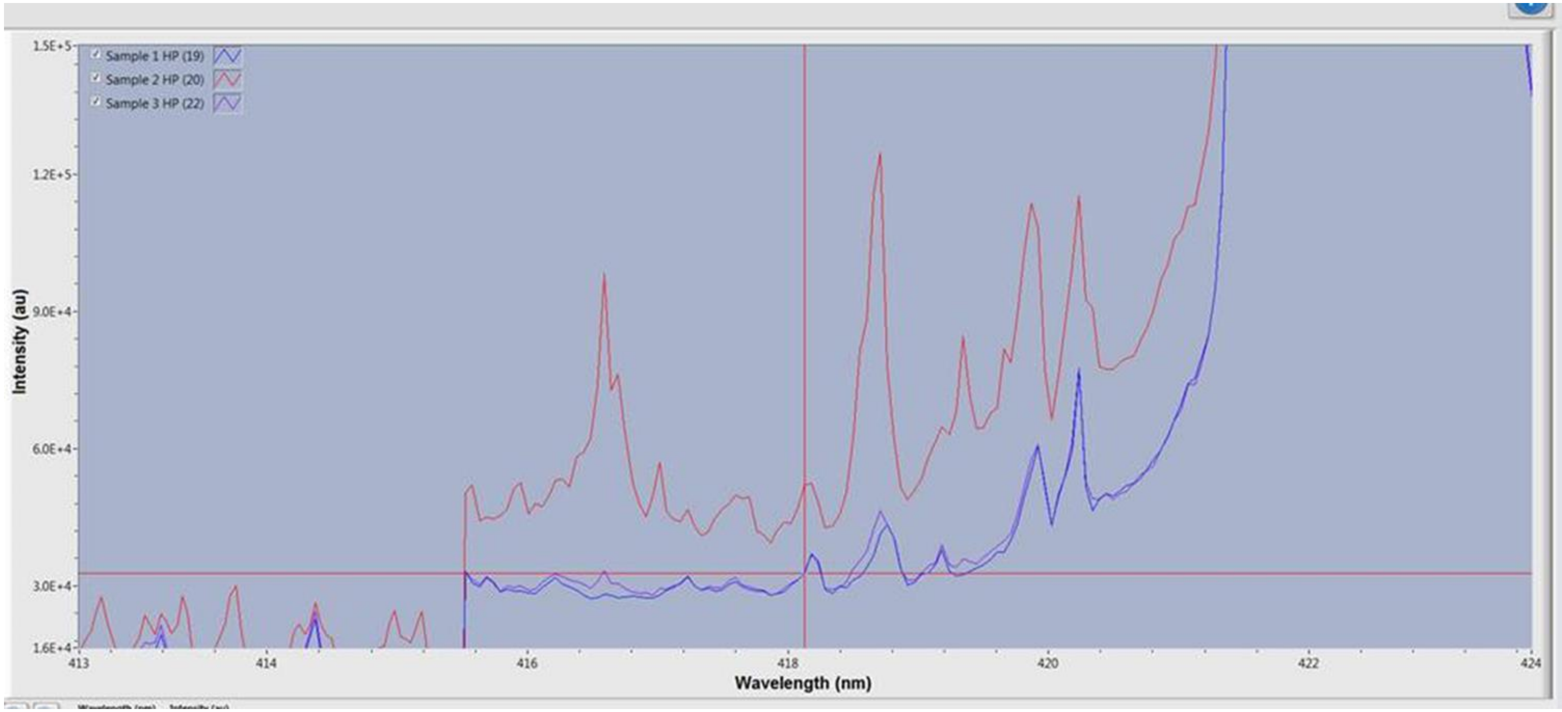

- Initial work shows possibility of using LIBS for contaminant detection.
- Further work on using nuclear simulant materials.
- Methods of contamination to be investigated – solid and liquid inclusions at mixing, immersion in contaminated water.

Thank you

Questions?

3D Real-time Reconstruction and Recognition for the Nuclear Waste on the Robot Arm

Henry Cheng Zhao[1], Kevin Li Sun[1] and Rustam Stolkin[1]
Tom Robinson[2]

University of Birmingham[1]
Birmingham, UK[1]
Sellafield Ltd[2]
Whitehaven, UK[2]

cxz514@cs.bham.ac.uk
lisunsir@gmail.com
R.Stolkin@cs.bham.ac.uk
tom.robinson@sellafieldsites.com

November 14, 2016

Contents

Robot Arm in Nuclear Industry

- Millions of technical wastes with radioactivity generated
- Improve the life safety and decrease the labour cost in the nuclear industry
- Automate the robot arm manipulation for the radioactive wastes classification, sorting and storing
- Make the robot arm have the abilities: 3D automatic reconstruction, 2D/3D nuclear material recognition and object manipulation in real-time

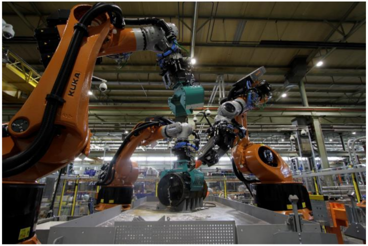

a

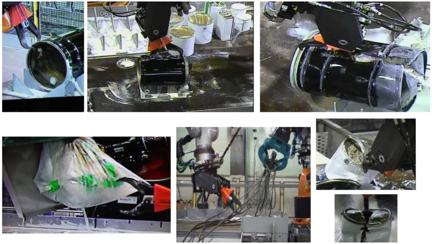

b

The Pipeline of RGBD SLAM

The pipeline of RGBD SLAM can be divided into two parts: Frontend and Backend.

Frontend: obtain the sensor data, extract the features and calculat the geometric relationships

Backend: construct a graph, perform loop closure detection, optimise the graph structure and generate the 3D map.

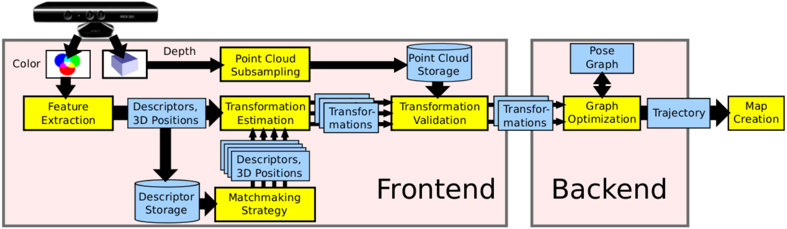

Figure: The pipeline of RGBD SLAM.

DISTINCTIVE UNIVERSITY OF BIRMINGHAM

The pseudo-code of RGBD SLAM

Algorithm 1 3D SLAM based on Graph Optimization

1: Initialize the key frame sequence F,
    add the first frame f_0 to F
    add $Vertex_{f_0}$ to $Graph$
2: **procedure** (For a new frame I, calculate the transformation e using SIFT based on RANSAC between the last key frame in F and I)
3:     **if** $Number_{goodmatch} < goodMatchThrehold$ **then**
4:         bad match, delete this frame.
5:     **if** $Number_{inliers} < inlierThrehold$ **then**
6:         bad match, delete this frame
7:     **if** $e > E_{far_t hreshold}$ **then**
8:         too far, delete this frame
9:     **if** $e < E_{key_t hreshold}$ **then**
10:         too near, delete this frame
11:     **if** $E_{key_t hreshold} \leqslant e \leqslant E_{far_t hreshold}$ **then**
12:         add I to key frame sequence F,
13:         add a $Vertex$ and a $Edge$ to $Graph$
14: **procedure** NEARBY LOOP DETECTION(compare the last N frames in F with I)
15:     **if** mactched **then**
16:         add a $Edge$ to the $Graph$.
17: **procedure** RANDOM LOOP DETECTION(compare the random N frames in F with I)
18:     **if** mactched **then**
19:         add a $Edge$ to the $Graph$.
20: **if** There is new frame **then**
21:     **goto** *Line 2*
22: **else**
23:     Optimize the pose
24:     Generate the 3D map

DISTINCTIVE UNIVERSITY OF BIRMINGHAM

3D Reconstruction Results

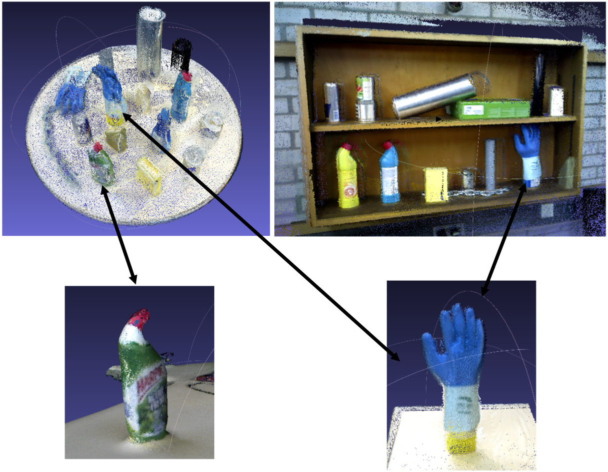

Figure: The 3D reconstruction results of the nuclear objects in a table and cabinet.

3D Reconstruction Results

Figure: The 3D reconstruction results of an office.

3D Reconstruction Demos

DISTINCTIVE UNIVERSITY OF BIRMINGHAM

3D Reconstruction Demos

1. Cabinet
2. Office
3. 3D models

DISTINCTIVE UNIVERSITY OF BIRMINGHAM

3D SLAM Evaluation

The error of 3D map is directly related to the error of the camera trajectory.
Relative pose error(RPE) and absolute trajectory error(ATE) for the visual odometry evaluation

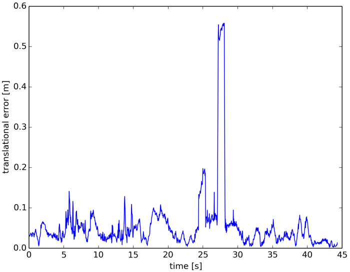

a

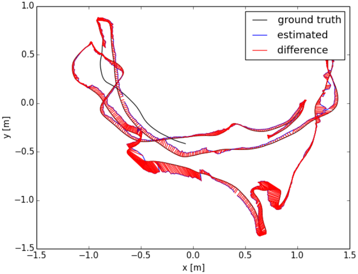

b

Figure: The plot of (a)RPE and (b)ATE of a office scene in TUM database.

DISTINCTIVE UNIVERSITY OF BIRMINGHAM

Materials in Context Database

Materials in Context Database (MINC) is employed for the CNN pre-training.
MINC has 23 different material data like wood, glass, metal, tile, leather, stone, paper, plastic, ceramic, fabric, brick, and etc.

Figure: The patches of 23 categories in MINC.

The Pipeline of Material Recognition

- Preprocess MINC data.
- Fine-tuning VGG network using MINC patches.
- Transplant VGG fully connected network into fully convolution network.
- Train FCN-32s, FCN-16s and FCN-8s network

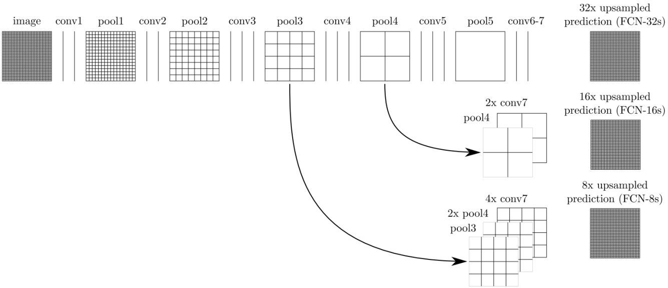

Figure: The pipeline of FCN-32s, FCN-16s and FCN-8s network.

The architecture of CNN

The architecture of fine-turning VGG, fully convolution network VGG, FCN-32s, FCN-16s and FCN-8s.

DISTINCTIVE UNIVERSITY OF BIRMINGHAM

The qualitative results

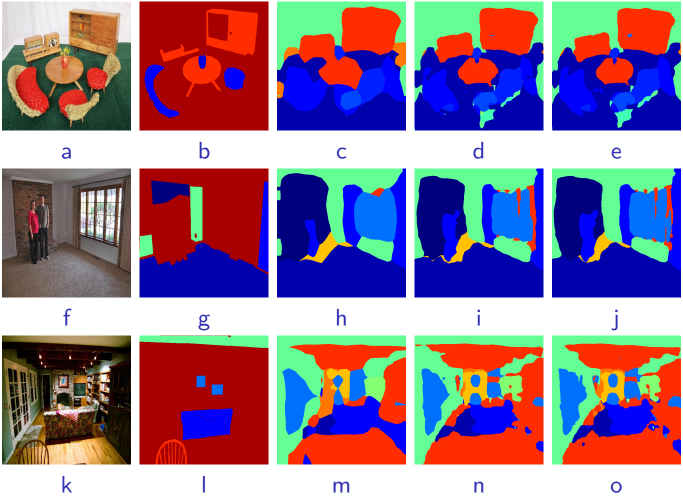

Figure: (1)original (2)Ground truth (3)FCN-32s (4)FCN-16s (5)FCN-8s

Material Recognition Demos

DISTINCTIVE UNIVERSITY OF BIRMINGHAM

Material Recognition Demos

1 Material recognition

DISTINCTIVE UNIVERSITY OF BIRMINGHAM

The quantitative results

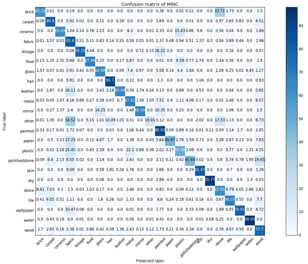

a

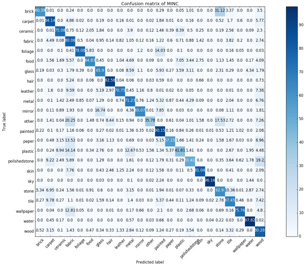

b

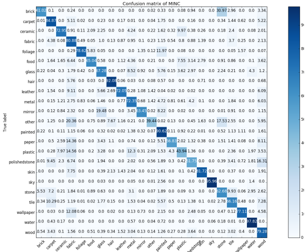

DISTINCTIVE UNIVERSITY OF BIRMINGHAM

Fast Object Detector

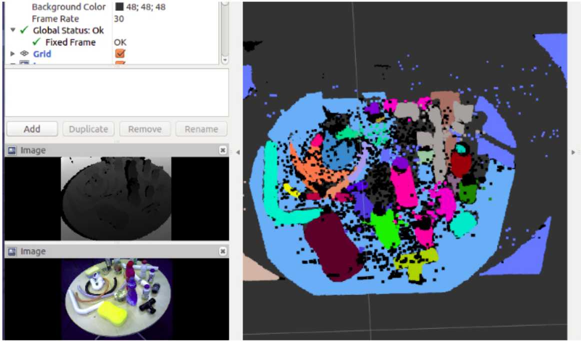

- Conditional Region Growth for Fast object detection

DISTINCTIVE UNIVERSITY OF BIRMINGHAM

Dataset Processing

- Pre-trained on ModelNet Dataset, 12k models
- virtual camera capture: 24 poses per object, 200+k depth maps

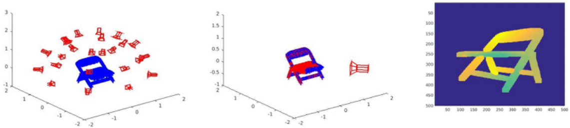

DISTINCTIVE UNIVERSITY OF BIRMINGHAM

Network Architecture

- 12 layers network architecture
- Scale-invariant: applying local region normalisation on features

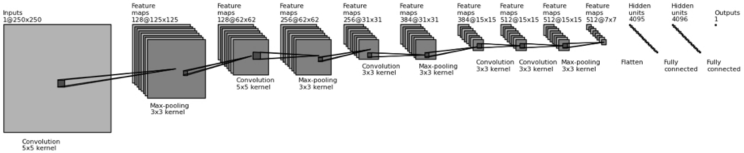

DISTINCTIVE UNIVERSITY OF BIRMINGHAM

Performance

- Average accuracy is 92.3% , second best in Model-Net dataset

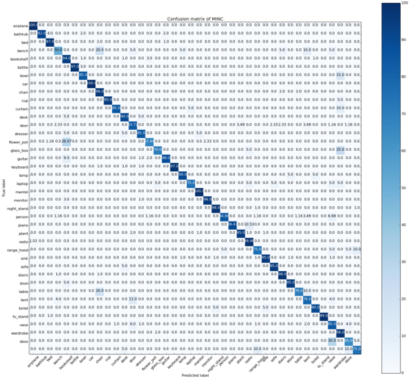

Algorithm	ModelNet40 Classification (Accuracy)	ModelNet40 Retrieval (mAP)	ModelNet10 Classification (Accuracy)	ModelNet10 Retrieval (mAP)
3D-GAN [10]	83.3%		91.0%	
VRN Ensemble [9]	95.54%		97.14%	
ORION [8]			93.8%	
FusionNet [7]	90.8%		93.11%	
Pairwise [6]	90.7%		92.8%	
MVCNN [3]	90.1%	79.5%		
GIFT [5]	83.10%	81.94%	92.35%	91.12%
VoxNet [2]	83%		92%	
DeepPano [4]	77.63%	76.81%	85.45%	84.18%
3DShapeNets [1]	77%	49.2%	83.5%	68.3%

Nuclear material database

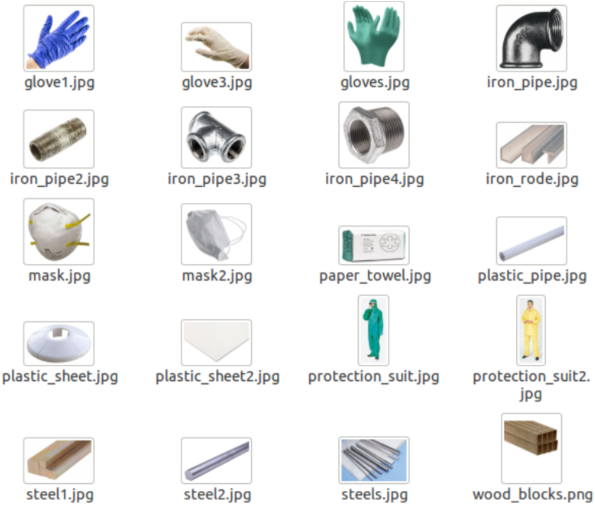

Figure: The nuclear material database.

DISTINCTIVE UNIVERSITY OF BIRMINGHAM

Future Work

Future work lists

1. Enlarge and diversify our nuclear industrial material database.
2. Optimize the 2D material recognition using CRF.
3. Integrate 3D reconstruction and 2D material recognition to 3D semantic reconstruction in real-time.
4. Apply the 3D real-time semantic reconstruction to the KUKA robot arm for nuclear waste picking and sorting.

Thanks.

Any questions?